Funnels, Pathways and the Energy Landscape of Protein Folding: A Synthesis

Joseph D. Bryngelson,
Physical Sciences Laboratory,
Division of Computer Research and Technology,
National Institutes of Health, Bethesda, MD 20892,

José Nelson Onuchic, Nicholas D. Socci,
Department of Physics-0319
University of California at San Diego
La Jolla, California 92093-0319

Peter G. Wolynes
School of Chemical Sciences and Beckman Institute,
University of Illinois,
Urbana, Illinois 61801

Abstract

The understanding, and even the description of protein folding is impeded by the complexity of the process. Much of this complexity can be described and understood by taking a statistical approach to the energetics of protein conformation, that is, to the energy landscape. The statistical energy landscape approach explains when and why unique behaviors, such as specific folding pathways, occur in some proteins and more generally explains the distinction between folding processes common to all sequences and those peculiar to individual sequences. This approach also gives new, quantitative insights into the interpretation of experiments and simulations of protein folding thermodynamics and kinetics. Specifically, the picture provides simple explanations for folding as a two-state first-order phase transition, for the origin of metastable collapsed unfolded states and for the curved Arrhenius plots observed in both laboratory experiments and discrete lattice simulations. The relation of these quantitative ideas to folding pathways, to uni-exponential *vs.* multi-exponential behavior in protein folding experiments and to the effect of mutations on folding is also discussed. The success of energy landscape ideas in protein structure prediction is also described. The use of the energy landscape approach for analyzing data is illustrated with a quantitative analysis of some recent simulations, and a qualitative analysis of experiments on the folding of three proteins. The work unifies several previously proposed ideas concerning the mechanism protein folding and delimits the regions of validity of these ideas under different thermodynamic conditions.

I Introduction

The apparent complexity of folded protein structures and the extraordinary diversity of conformational states of unfolded proteins makes challenging even the description of protein folding in atomistic terms. Soon after Anfinsen's classic experiments on renaturation of unfolded proteins [1], Levinthal recognized the conceptual difficulty of a molecule searching at random through the cosmologically large number of unfolded configurations to find the folded structure in a biologically relevant time [2]. To resolve this "paradox," he postulated the notion of a protein folding pathway. The search for such a pathway is often stated as the motive for experimental protein folding studies. On the other hand, the existence of multiple parallel paths to the folded state has been occasionally invoked [3]. Recently, a new approach to thinking about protein folding and about these issues specifically has emerged based on the statistical characterization of the energy landscape of folding proteins [4–6].

This paper presents the basic ideas of the statistical energy landscape view of protein folding and relates them to the older languages of protein folding pathways. The use of statistics to describe protein physical chemistry is quite natural, even though each protein has a specific sequence, structure and function essential to its biological activity. The huge number of conformational states immediately both allows and requires a statistical characterization. In addition folding is a general behavior common to a large ensemble of biological molecules. Many different sequences fold to essentially the same structure as witnessed by the extreme dissimilarities in sequence which may be found in families of proteins such as

1

lysozyme [7]. Thus for any given observed protein tertiary structure, there is a statistical ensemble of biological molecules which fold to it. Many studies suggest that the dynamics of many parts of the folding process are common to all of the sequences of a given overall structure, while others are peculiar to individual sequences. *Distinguishing folding processes common to all sequences from those peculiar to individual sequences is a major goal of physical theories of protein folding.* The statistical energy landscape analysis will show which features are common and which are specific taxonomic aspects of protein folding.

Depending on the statistical characteristics of the energy landscape, either a unique folding pathway or multiple pathways may emerge. A biological relevance of the distinction between the two pictures is that mutations can more dramatically affect the dynamics through unique pathways than through multiple pathways.

The organization of this paper is as follows: in the next section we describe the energy landscape of protein folding, discuss the properties of smooth and rough energy landscapes, and indicate that it appears that protein folding occurs on an energy landscape that is intermediate between most smooth and most rough. In Section Three, we describe a simple protein folding model that interpolates between these two limits and exhibits both the smooth and the rough energy landscape properties that are present in folding proteins. The equilibrium thermodynamic properties of this model are also discussed in this section. Section Four starts with a short survey of the differences between the kinetics of complex chemical processes, such as protein folding, and the kinetics of the simple chemical processes whose understanding forms the basis of the most commonly used reaction rate theories. We review how these common theories should be modified to cope with the complexity of a process like protein folding. Then we present the necessary modifications of kinetics and apply them to the simple protein folding model of Section Three. Each scenario has its own characteristic behavior. The folding scenario observed in any given experiment depends on the specific sequence and the refolding conditions. Section Five shows how the scenarios presented in Section Four can be understood in terms of the phase diagram for protein folding. This phase diagram is also discussed in detail. In the next section we show how the energy landscape ideas can be used to analyze data by presenting a rough but quantitative analysis of some computer simulation data. In the following section, Section Seven, we give a flavor of the issues in energy landscape analysis of experimental data through an examination of some previously published experimental results. We also present a tentative assignment of the folding scenarios observed in these experiments. The concluding section then summarizes the results, and discusses the significance of the energy landscape for understanding protein folding, for protein structure prediction and for protein engineering.

II   Smoothness, Roughness and the Topography of Energy Landscapes

Protein folding is a complex process, typically occurring at a constant pressure and temperature, involving important changes in the structure of both the chain and the solvent [8, 9]. The natural thermodynamic potential for describing processes at constant pressure and temperature is the Gibbs free energy [10, 11], so we will use an effective free energy that is a function of the configuration of the protein to describe the protein-solvent system. Notice that this description implicitly averages over the solvent coordinates. This averaging means

2

that the forces that arise from this potential function are temperature dependent. To make these considerations more concrete, consider the forces on two apolar groups immersed in water. The apolar-group-solvent-system has a lower free energy if the two apolar groups are close to one another, so the solvent-averaged free energy, mentioned above, has a minimum when the two groups are close and becomes larger when the groups are further apart [12]. The change in the solvent-averaged free energy as a function of distance between the groups causes the groups to attract one another. This attraction is the hydrophobic force. Since the free energy of the apolar-group-solvent-system changes as the temperature changes, likewise the solvent-averaged free energy and the hydrophobic force also change [12, 13].

The need to consider the form of the free energy as a function of protein conformation, which we call the energy landscape, stems, in part, from a well-known argument of Cyrus Levinthal [2]. The argument starts by noticing that number of possible conformations in a protein scales exponentially with the number of amino acid residues. Thus, if each amino acid has only two possible conformations, then the number of possible conformations for a protein with 100 amino acid is $2^{100} \approx 10^{30}$. If, as a conservative estimate, at least one picosecond is required to explore each conformation, then the time required to explore all conformations of the 100 amino acid protein is approximately 10^{18} seconds, or more than 10^{10} *years*. From this estimate Levinthal argued that the protein did not have enough time to find its global free energy minimum, so the final, folded conformation of a protein must be determined by kinetic pathways. This argument is easily criticized. For example, one could equally well apply it to the formation of crystals, and conclude that crystallization can never occur! More seriously, the argument can be used to question how the protein could reliably find *any* particular conformation. In this form the argument is often called Levinthal's paradox. The weak point in Levinthal's argument is the assumption that all conformations are equally likely in the path from the unfolded to the folded states. In fact, conformations with lower free energy are more likely than those with higher free energy. Levinthal's argument assumes a free energy landscape that looks like a flat golf course with a single hole at the free energy minimum. The argument breaks down completely for a free energy landscape that looks like a funnel [5, 14–16]. A central purpose of this paper is to further develop this intuitive notion of energy landscape and to describe quantitatively kinetic behavior on the kinds of energy landscapes that are encountered in protein folding. Interestingly, Levinthal's paradox will reoccur, albeit in a completely different form.

The most detailed description of the energy landscape of a folding protein molecule would be obtained by specifying the free energy averaged over the solvent coordinates as a function of the coordinates of every atom in the protein. At this fine level of description, the free energy surface of a protein is riddled with many local minima [17, 18]. Most of these minima correspond to small excitation energies connected with individual local conformational changes such as rotations of individual side chains. The energies involved in these small conformational changes are typically on the order of $k_B T$, that is, the size of the thermal energies of the atoms in the protein. Interconversion between these shallow local minima will be rapid on the time scale of protein motions. Sometimes many sidechains can shift, giving quite different minima with a large energy barrier between them. Changes of backbone conformation can lead to globally different protein folds involving many different inter-residue contacts. The energies involved in these larger conformational differences can easily become

many times k_BT, and interconversion between these deeper, globally different local minima can be quite slow [17, 18].

The interesting features of protein folding dynamics concern the free energy surface viewed on this more coarse-grained structural scale. Very different behavior occurs, depending on whether this coarse-grained energy landscape is "smooth" or "rough." In Figure 1 we show representative smooth and rough energy landscapes. A smooth energy landscape has only a small number of deep valleys and/or high hills. For smoother energy landscapes there are typically many high energy structures and only a few low energy structures. The more closely the system resembles a few low energy structures, the lower the energy. Thus, each of the low energy structures is at the bottom of a broad energy valley. A protein molecule that was in one of the valleys would find itself dynamically funneled to the lowest energy state. Therefore, we will refer to the valley associated with a low energy structure a "funnel". In this language, a system with a smooth energy landscape has a few deep minima, each having a large, broad funnel. Systems with smooth landscapes exhibit cooperative phase transitions, illustrated by such phenomena as crystallization of simple materials and in biological macromolecules by phenomena such as the helix-coil transition [19]. The thermodynamic phases of systems as smooth energy landscapes are determined by the temperature. At high temperatures, the large number of high energy structures predominate, but as the temperature of the system is lowered, the system will occupy the lower energy states. Dynamically, below a transition temperature, such systems will fall into a funnel of low energy states and may remain trapped there. In typical cooperative transitions such as crystallization, once a large enough nucleus of low energy structure is formed, the rest of the low energy structure forms rapidly [20–22].

Thermodynamically, protein tertiary structure formation for smaller proteins has been shown to exhibit this type of cooperative behavior. For small, single domain proteins, at most two states are observed on the longest time scales under physiological solvent conditions: One a high entropy high energy disordered phase corresponding to the unfolded protein, and a lower entropy low energy phase describing the folded protein [23]. The fact that the phase space is divided into two main parts is confirmed by the coincidence of transitions measured by different probes such as optical rotation or fluorescence [24–26]. In addition on the longest time scales, one sees only a single exponential in the kinetics of folding. Simulations of protein folding have shown evidence of nucleation-like behavior [27]. Thus these aspects of tertiary structure formation are characteristic of a system with smooth energy landscape.

Smooth energy landscapes are so commonly used in the description of problems that systems with rough energy landscapes are considered exotic and have only recently been studied by chemists and physicists. A rough energy landscape would be one that when coarse grained has many deep valleys and very high barriers between them. In such a rough energy landscape there are very large numbers of low energy structures that are entirely different globally. Each of these diverse low energy structures has a small funnel leading to it.

The thermodynamic and kinetic behavior of systems having rough energy landscapes is quite distinct from those with smooth landscapes. Rough energy landscapes occur in problems in which there are many competing interactions in the energy function. This competition is called "frustration." The paradigm for a frustrated system is the spin glass, a

Figure 1: The energy of a system (vertical axis) is sketched against a single coordinate (horizontal axis) for representative smooth and rough energy landscapes. The top sketch shows a smooth landscape with only a few energy minima each having a broad funnel leading to it. The bottom sketch shows a rough energy landscape with many energy minima each with a narrow funnel leading to it.

magnetic system in which spins are randomly arrayed in a dilute alloy [28–30]. The interactions between spins are equally often, at random ferromagnetic (the spins want to point in the same direction) and antiferromagnetic (the spins want to point in opposite directions). These two conflicting local tendencies (one to parallel spins, the other to alternating spins) can not be satisfied completely in any arrangement of spin orientations. Thus, the system is said to be "frustrated" [31]. Many optimization problems that arise in economic contexts have rough energy landscapes because of frustrated interactions. An economic example of a rough landscape is provided by the traveling salesman problem. In this problem one attempts to minimize the total length of a journey which visits each of a set of randomly arrayed cities precisely once during the trip. Here searching for the minimum length trips leads to an optimization problem in which there are many alternate routes that have very nearly the same value of the required length (equivalent to multiple minima). The frustration here arises from the constraint of a single visit to a city because of an occupancy tax; no central location can be used as a base. Finding the optimal solutions to this problem is a difficult task. Computer scientists have developed a set of ideas that describes many problems that are hard to solve [32]. Although the precise technical framework of these ideas is elaborate, the basic idea is simple; there exists a set of difficult problems that can not be solved by any known polynomial time algorithm, and it is generally believed that no such algorithm exists. These problems are called NP-complete. Here by polynomial time algorithm we mean that the amount of computation time required to solve the problem grows no faster than some fixed power of the problem size, $e.g.$, the number of cities in the traveling salesman problem. Furthermore, the general model of computation used in NP-completeness proofs is thought to be able to simulate any natural system, so the limitations that NP-completeness impose on computation probably hold for all natural systems, $e.g.$, folding proteins, the human brain, $etc.$. Thus, solutions to NP-complete problems require an exponential, rather than polynomial, amount of time. In practical terms, NP-completeness means that the amount of time required to solve even modest size problems can become astronomically large. The traveling salesman problem an example of a NP complete problem; that is, its solution for the general case requires exponentially more computational time as the size of the problem grows. Finding the lowest free energy state of a macromolecule with a general sequence also been shown to be NP-complete [33]. NP-completeness is a worst case analysis; if a problem is proven to be NP-complete then finding the solution to at least one case requires an exponential computation time. In economic situations these computational difficulties are avoided by choosing to be satisfied with an acceptable solution or by selecting the conditions of the problem so that easy answers can be found. An example of the latter is the introduction of the "hub" system to airline traffic. A central city, perhaps not usually visited, is introduced as a place that can be multiply visited at little cost. Similarly for the physicist's spin glass, there are some specifically chosen arrangements of ferromagnetic and antiferromagnetic interactions so that each interaction can be satisfied in a single configuration. The arrangements of interactions which do this are relatively improbable. Therefore, in the context of proteins, NP-completeness means that there are amino acid sequences that can not be folded to their global free energy minimum in a reasonable time either by computer or by the special algorithm used by Nature. Thus, in analogy with the economic situation, either naturally occurring proteins fold to a structure that is not a global minimum or they

have been selected to be members of the subset of amino acid sequences that *can* fold to their global free energy minimum in a reasonable time. The NP-completeness proof does alone not distinguish between these two possibilities. If the latter possibility is correct then one approach to predicting structure is simulated annealing [34]. Starting at high temperatures, the system is slowly brought to low temperature while following its dynamics. These stochastic search algorithms parallel the Levinthal paradox for protein folding kinetics. Such an approach can only work if the computers energy landscape is sufficiently close to the one that Nature used.

In any case, even if proteins fold to a structure that is not a global minimum, *i.e.*, folding is kinetically controlled, they must *reliably* fold to a single structure. Recent experiments on random and designed amino acid sequences have shown that reliable folding is not a universal property of polypeptide chains, and that multiple folded structures are the rule rather that the exception [35, 36]. Thus, both theory and experimental evidence indicate that such reliable folding is characterizes only a small fraction of amino acid sequences. Proteins are a subset of this fraction of reliable folders. Later in this paper we discuss a property we call minimal frustration. Evidence from theory and from simulation indicates that amino acid sequences with minimal frustration are likely to fold reliably.

What are the possible sources of frustration in the general case of a heteropolymer? Consider the hydrophobic effect, which for illustration we think of as a contact interaction favoring hydrophobic pairs or hydrophilic pairs. Because of the constraint of chain connectivity for most random sequences bringing together a hydrophobic pair distant in sequence will require bringing together other pairs in the sequence which will often be dissimilar and therefore unfavorable.[1] This situation could be avoided in natural proteins by choosing simple patterns of hydrophobic-hydrophilic alternation like those seen in β-barrel proteins [37]. Similarly, for most sequences the hydrophobicity pattern favoring a particular secondary structure (α-helix or β-sheet) might or might not be consistent with the tendency of each amino acid to be in that secondary structure. Indeed, in general is usually some conflict of this sort, since the ends of α-helices have unsatisfied hydrogen bonds, but the helices must be broken so that a compact structure can form, satisfying the hydrophobic forces. Sequences may need special start or stop residues to form terminal hydrogen bonds gracefully, using sidechains [38, 39].

Polymers can also exhibit another kind of frustration. A molecule often needs to overcome an energy barrier to change from one structure to another. This notion has been used explicitly in the simulation studies of Camacho and Thirumalai and of Chan and Dill where they constructed paths with minimal energy barriers between similar configurations in their protein folding models and used this network of pathways to map out several features of the energy landscape [40–42]. If this energy barrier is too high to overcome in a reasonable time, for example, some fraction of the folding time for a protein, then we may say that the two structures are not "dynamically connected". Two different structures may resemble each other, and even have similar free energies, but they may be unable reconfigure from one to the other one in any reasonable time scale. Such structures would not be dynamically

---

[1]It is useful for the reader to study Figure 2, in which we illustrate the varying degrees of frustration for two sequences of a lattice model of a heteropolymer.
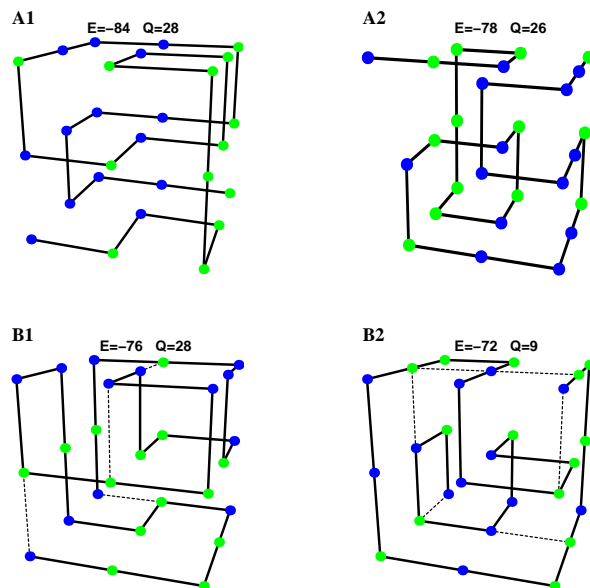
Figure 2: The ground state of two different sequences for a 27-mer, with two different types of monomers (two letter code) on a cubic lattice. If two monomers are adjacent in space, but not along the chain, then there is an attractive interaction between them. This interaction is strong if the monomers are of the same type and weak if they are of different types. For all figures we use the following notation: solid lines represent covalent bonds, dashed lines represent spatial contacts with weak interactions and no lines are drawn for spatial contacts with strong interactions. The model for this 27-mer is presented fully in section 6. The strong interactions are equal to -3 and the weak ones to -1 in an arbitrary energy units. The most compact configurations will be cube-like and they have 28 spatial (non-bonded) contacts. Sequence (A) has only strong contacts in its ground state. For this reason we call it a non-frustrated ground state. Figure A1 shows the ground state structure for this sequence. We call it non-frustrated because all contacts are optimal. We show in Section 6 that this sequence is a good folding sequence. This is not the case for sequence (B). Its ground state configuration has 4 weak interactions, as shown in Figure B1. For this reason we say that this sequence is frustrated, *i.e.*, it is unable to optimize all the interactions and it has to compromise with some weak ones. We show in section 6 that sequence (B) is not a good folder. However, there is a more interesting way of observing frustration. Let us call Q a measure of similarity between the ground state configuration and any other configuration (compact or non-compact) for a given sequence. The quantity Q measures the number of contacts between pair of residues that are the same for a given configuration and its ground state one. Therefore, Q is a number between 0 and 28. Most of the configurations with energy just above the ground state in sequence (A) have Q between 18 and 26, *i.e.*, very similar to the ground state configuration. An example of such a configuration is shown in Figure A2 where the energy is -78 and Q is 26. The situation is completely different for sequence (B). There are configurations with energy just above the ground state configuration that have a Q between 4 and 12, *i.e.*, they are very different from the ground state. An example of one of these configurations is shown in Figure B2 where the energy is -72 and Q is 9. In this case, there are lots of low energy states that are completely different but energetically very similar. When the system gets trapped in one of these low energy states, it takes a long time to completely reconfigure before it can try to fold again.

connected. In particular, for polymers, geometrical constraints arise because the polymer chain can not pass through itself. This effect is called excluded volume, and may give rise to an enormous energy barrier. In this case one can easily have two structures that resemble each other but are not dynamically connected. Leopold, Montal and Onuchic have explicitly shown that this situation occurs in some simple models of protein folding [15]. We will refer to this kinetic phenomenon as geometrical frustration.

Systems with rough energy landscapes also exhibit effective phase transitions [28–30]. When the temperature of such a system is lowered, it tends to occupy the lower energy states and at a transition temperature will become trapped in one of them. Generally, these transitions are accompanied by a considerable slowing of the motion as the system tries to exit over the high energy barriers. In the case of liquids being super–cooled below their freezing point, this phenomenon is known as the glass transition [43, 44]. Below the glass transition temperature, the liquid is trapped in a single deep minimum and thus it looks like a solid. The thermodynamics of this solid depends on its detailed thermal history. Typically, systems with rough energy landscapes exhibit glass transitions analogous to those that occur when liquids are supercooled below their freezing point. As the system approaches the glass transition, the slow transitions between minima leads to strongly non–exponential time dependence for many properties.

Typically a heteropolymer with a random sequence interacting with itself has a rough energy landscape. One source of the roughness is the frustration arising from conflicting interactions but geometrical constraints may be important too. In either case, energetic or geometrical frustration, there will be a large barrier to reconfigure between these configurations. This is a natural starting assumption for thinking about heteropolymer dynamics since one expects this behavior generically for heterogeneous systems. The implications of the roughness of heteropolymer energy landscapes for protein folding were first discussed by Bryngelson and Wolynes who postulated that the energies of the states of a random heteropolymer could be approximately modeled by a set of random, independent energies [4]. This model is known as the random energy model in the theory of spin glasses [45–47]. The random energy model approximation used by Bryngelson and Wolynes was later shown to be equivalent to a more conventional replica mean field approximation by Garel and Orland [48] and by Shakhnovich and Gutin [49]. A direct demonstration of the roughness of the energy landscape for heteropolymers has been carried out for small lattice model proteins. Here the exact enumeration of configurations can be carried out and with simple interactions, it can be directly established that there are configurations very close in energy to the ground state that have topologically distinct folds for most random sequences [50–55]. Work on realistic lattice models for small proteins confined to their proper shape (where complete enumeration can be carried out) suggests the possibility of deep low energy structures that are globally different in form [56, 57]. Even for a well designed sequence (*i.e.* one designed to have a smooth energy landscape) some roughness may remain. Early direct evidence for roughness in the energy landscape of protein folding simulations of designed sequences is provided by the work of Honeycutt and Thirumalai, which looked for and found deep multiple energy minima in their simulations of β-barrel folding [58, 59]. Finally, the historical difficulty of predicting protein structure from sequence arises from the "multiple minimum problem," that is, the existence of many minima in the empirical potential energy functions used to

predict these structures. The large number of minima indicates that the energy landscape of these potential functions is rough. The importance of the multiple minimum problem, and therefore the roughness of the energy landscape, as an impediment to structure prediction has been emphasized by Scheraga and collaborators [60].

Some experimental features of protein folding suggest a considerable roughness to the energy landscape. Although protein folding appears to be exponential in time, short time scale measurements show the existence of intermediates. Also, multi-exponential decay of relaxation properties are seen in these early events [61]. Many of the time scales involved in protein unfolding have very large apparent activation energies, suggesting high energy barriers. There is the occasional report of history dependence to protein folding; although, this is absent from studies on smaller proteins *in vitro* [23].

III Quantitative Aspects of the Statistics and Thermodynamics of A Folding Protein.

In the previous section we found that a folding protein exhibits behaviors that are characteristic of both smooth and rough energy landscapes. Thus, from the phenomenological viewpoint it is evident that protein folding occurs on an energy landscape that is intermediate between the most smooth and the most rough. A simple model proposed by Bryngelson and Wolynes interpolates between the two limits and illustrates the basic ideas of the energy[2] landscape analysis of protein folding [4]. When stripped down to its bare essentials, this picture of the folding landscape is based on two postulates: The first captures the rough aspects of the energy landscape. It is postulated that (for natural proteins) the energy of a contact between two residues which does not occur in the final native structure of a protein or the energy of a residue in a secondary structure which does not turn out to be ultimately correct can be taken as random variables; that is, in its non-native interactions, a protein resembles a random heteropolymer. In its extreme form this suggests that we can take the energies of globally distinct states to be random variables which are uncorrelated, provided no native contacts are made and no native secondary structure is formed. A second postulate captures the smooth aspects of the folding landscape. When a part of the protein molecule is in its correct secondary structure, the energy contributions are expected to be stabilizing. In addition, when a correct contact is made, although occasionally the energy may go up, on the average over all possible contacts, the energy will go down. Thus if the similarity to the native structure is used as a distance measure, the surface may have bumps and wiggles but the energy generally rises as we move away from the native structure. Thus there is an overall energetic funnel (of the sort discussed in the previous section) to the native structure.

Bryngelson and Wolynes used the term the principle of minimal frustration in describing the smoothness postulate, insofar as it is what distinguishes natural proteins from random heteropolymers. The smoothness of folding landscapes arises from the selection of protein

---

[2]In this section we use the word "energy" to describe the free energy of a given complete configuration of the protein. such a configuration has many solvent configurations consistent with it. Thus our energy landscape has a temperature dependence due to hydrophobic forces. We do not consider this effect when we discuss the pure effects of temperature in this section.

sequences by evolution. If the necessity to maximize the ability of folding quickly is the dominant selection pressure, the smooth part of the energy landscape will be paramount. On the other hand, there are other selection pressures as well. Thus evolution may not be able to remove some frustrated interaction from natural proteins. Indeed, neutral evolution would suggest that randomness and frustration would continue to exist to an extent that allows only adequate stability and kinetic foldability. The minimal frustration of natural proteins is evident in several ways. Examination of X-ray structures shows that sidechains are in fact chosen by evolution to make coherent contributions to supersecondary structures. Clear examples are leucine zippers [62] and the β-barrel amphiphilicity mentioned earlier. Symmetric sequences like these often lead to low frustration in symmetric structures. Consistency between secondary structures and global tertiary structures is also important. This is the "principle of structural consistency" enunciated by Gō [63].

Purely kinetic effects also limit the folding of proteins. For example, if the minimum energy structure is not dynamically connected (in the sense described in the previous section) to any other low energy structures, then it would be kinetically inaccessible in spite of its low energy. The importance of kinetic effects for protein folding was investigated in the previously mentioned study of Leopold, Montal, and Onuchic [15]. They simulated the folding of two "sequences" with their simple model, one of which folded rapidly to its global energy minimum, the other of which failed to find its global energy minimum in several long runs. Analysis of the dynamical connectivities produced by the two "sequences" showed that the minimum energy structure of the rapidly folding sequence had a rich network of dynamical connections to most of the other low energy structures. In contrast, the minimum energy structure of the other sequence was sparsely connected to other low energy structures.

A figure encompassing the qualitative considerations about the folding landscape is pictured in Figure 3a. Of course, no low dimensional figure can do justice to the high dimensionality of the configuration space of a protein, but one sees that the dominant smooth features of the landscape depend on how close a protein configuration is to the native one and this coordinate is specifically shown as the radial coordinate in the figure. There are a variety of ways of measuring the similarity of a protein structure to the native structure. One can take the fraction of the amino acids residues which are in the correct local configuration. This is a choice used in the original papers of Bryngelson and Wolynes [4–6]. Another possibility for measuring tertiary structure is the fraction of pairs of amino acids which are correctly situated to some accuracy. This measure is related to the distance plots used by crystallographers [64, 65]. The similarity measure may also be thought of as a measure of the distance between the two structures, so that similar structures are considered to be close to one another. We denote the similarity of a protein structure to the native structure by n. We will take $n = 1$ to denote complete similarity to the native state and $n = 0$ to denote no similarity to the native state. The radial coordinate in Figure 3a should be thought of as this similarity measure n. The average energy of state with a certain similarity to the native structure has a value that gets lower as the native structure is approached - thus the overall slope of the energetic funnel. On the other hand the rugged part of the energy landscape means that no individual state has precisely this energy and we can characterize the fluctuations in energy with a given similarity to the native structure by the variance, $\Delta E^2(n)$. The ruggedness of the energy landscape as measured by this variance clearly depends on the
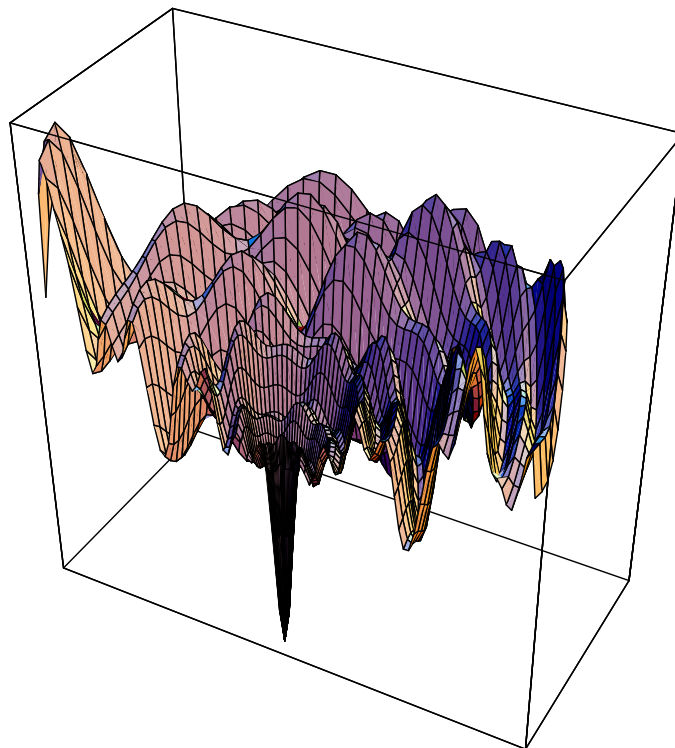
Figure 3: (a) Sketch of an energy landscape encompassing the qualitative considerations about the folding. The energy is on the vertical axis and the other axes represent conformation. This landscape has both smooth and rough aspects. Overall, there is a broad, smooth funnel leading to the native state, but there is also some roughness superimposed on this funnel. Of course, no low dimensional figure can do justice to the high dimensionality of the configuration space of a protein.

compactness of the protein molecule since it arises from improper 3-dimensional contacts. In general, the variance may also conceivably decrease as the native structure is approached, but this is not essential for our picture.

The energy of a given state arises from the contributions of many terms, so it is natural to assume that the probability distribution of energies for any similarity to the native structure is given by a Gaussian distribution,

$$P(E) = \frac{1}{\sqrt{2\pi\Delta E^2(n)}} \exp{-\frac{\left(E - \bar{E}(n)\right)^2}{2\Delta E^2(n)}}. \tag{1}$$

The other important feature of the statistical landscape description is the number of conformational states of protein as we move away from the native structure. The total number of conformational states grows exponentially with the length of the protein. If there are γ configurations per residue, this total number of configurations is $\Omega = \gamma^N$. γ depends on the level of description of the model. It is of order 3, 4 or 5 for the backbone coordinates, but might rise to roughly 10 if the sidechain configurations are also included in the analysis. As noted above, the ruggedness of the energy landscape is most important when the protein is compact. The number of compact configurations is considerably smaller than the total number and can be estimated from Flory's theory of excluded volume in polymers [66, 67], $\Omega(R)$ decreases quite considerably as the radius of gyration of the protein falls. For maximally compact configurations of the backbone, $\Omega(R)^* = \gamma^{*N}$ where γ^* is of the order 1.5.

The completely folded protein has a much smaller degree of conformational freedom. Essentially a single backbone structure exists. Thus the number of configurations of the protein decreases as we move toward the native structure. Therefore, if $\Omega(n)$ denotes the number of structures with a similarity measure with the native structure of n, then $\Omega(n)$, and

$$S_0(n) = k_B log\Omega(n) \tag{2}$$

decreases as n gets larger. The exact similarity measure determines the behavior of $S_0(n)$. For our purposes here we need only take a simple form of $S_0(n)$ that decreases as the native state is approached. Roughly speaking, we can approximate Ω as a function of n by $\Omega = \gamma^{*N(1-n)}$.

As one moves away from the native structure there is a huge increase in the number of accessible states, which we can think of as living on the branches of a highly arborized tree as is shown schematically in Figure 3b. Not all of the states on a statistical landscape are thermodynamically or kinetically important, since the high energy states cannot be thermally occupied. The number of states with a specified energy E, which have a specified similarity, n, to the native structure, is given by

$$\Omega(E, n) = \gamma^{*N(1-n)}P(E) . \tag{3}$$

At thermal equilibrium, only a small band of energy is occupied with a certain similarity to the native structure. For a large protein, this band will be relatively well defined in energy. The most probable value of the energy in this band can be obtained by maximizing
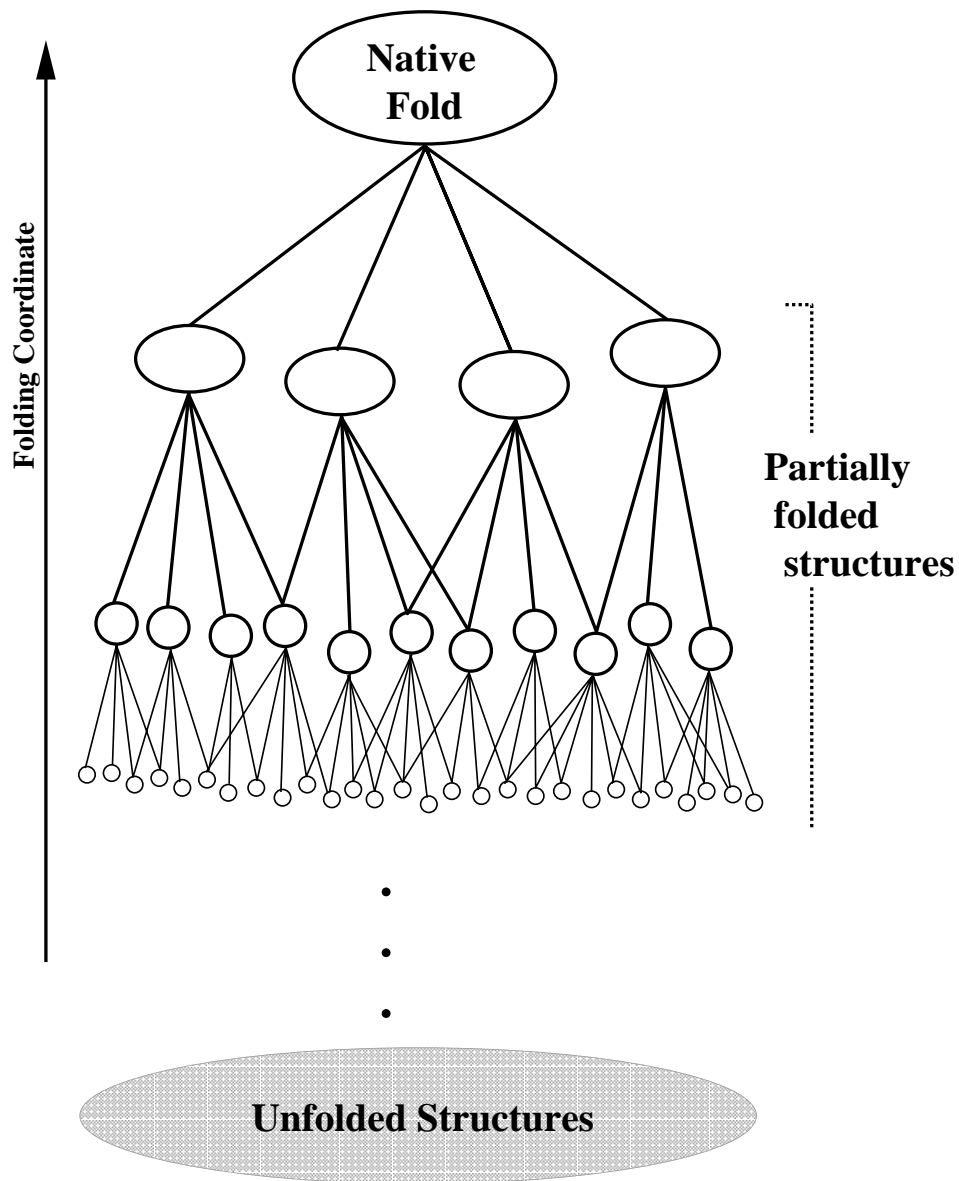
Figure 3: (b) A schematic drawing of protein conformations in relation to their similarity to the native state. The vertical direction is a folding reaction coordinate. The conformations that are higher in the figure are more similar to the native state. As one moves away from the native structure there is a huge increase in the number of possible conformations.

the thermodynamic weight of states of a given energy. This is a product of the Boltzmann factor and the number of states of that energy

$$p(E, n) = \frac{1}{Z} \Omega(E, n) e^{-E/k_B T} . \tag{4}$$

(Note: Do not confuse $p(E)$ above with the $P(E)$ defined in equation 1.) Here Z is the partition function, which ensures normalization of the probability function. Thus the most probable energy with a certain similarity to the native structure is given by

$$E_{m.p.}(n) = \bar{E}(n) - \frac{\Delta E(n)^2}{k_B T} , \tag{5}$$

and the number of thermally occupied states is

$$\Omega(E_{m.p.}(n), n) = \exp\left[\frac{S_0(n)}{k_B} - \frac{\Delta E(n)^2}{2(k_B T)^2} \right] \tag{6}$$

The entropy of the thermally occupied structures that have a certain similarity to the native structure is,

$$S(E_{m.p.}(n), n) = k_B \log(\Omega(E_{m.p.}(n), n)). \tag{7}$$

We see from these expressions that there are two opposing thermodynamic forces involved in the folding process. The growth in the number of thermally occupied states as we move away from the native structure favors a large number of highly disordered configurations. On the other hand, the decreasing average energy as one approaches the native structure favors folded configurations. These two features are combined by thinking of the free energy as a function of the configurational similarity n at a fixed temperature T,

$$\begin{aligned} F(n) &= E_{m.p.}(n) - TS(E_{m.p.}(n), n) \\ &= \overline{E}(n) - \frac{\Delta E(n)^2}{2k_B T} - TS_0(n) . \end{aligned} \tag{8}$$

This free energy function is the logarithm of the thermodynamic weight of states with a certain similarity to the native structure. We see in Figure 4 a representation of this free energy and of the probability of occupation. At high temperatures, the band of states with nearly no native structure is favored, corresponding to an unfolded state. At very low temperatures the folded configurations would be favored and in between, a double minimum effective free energy pertains. The folding temperature is determined by the condition that the two global minima be equal in thermodynamic weight. The unfolded minimum can correspond to two distinct sets of states corresponding to different values of a distinct order parameter, the radius of gyration [6]. If the randomness is large and non-specific interactions are important, or the chain is highly hydrophobic in composition, this minimum itself can be collapsed. This may well correspond to the molten globule state [68]. On the other hand, if there is little average driving force to collapse due to non-specific contacts ($\Delta E(n)^2$ small) the disordered configurations will non-compact and this corresponds to the traditional denatured random coil state. We note that many intermediate degrees of order can exist
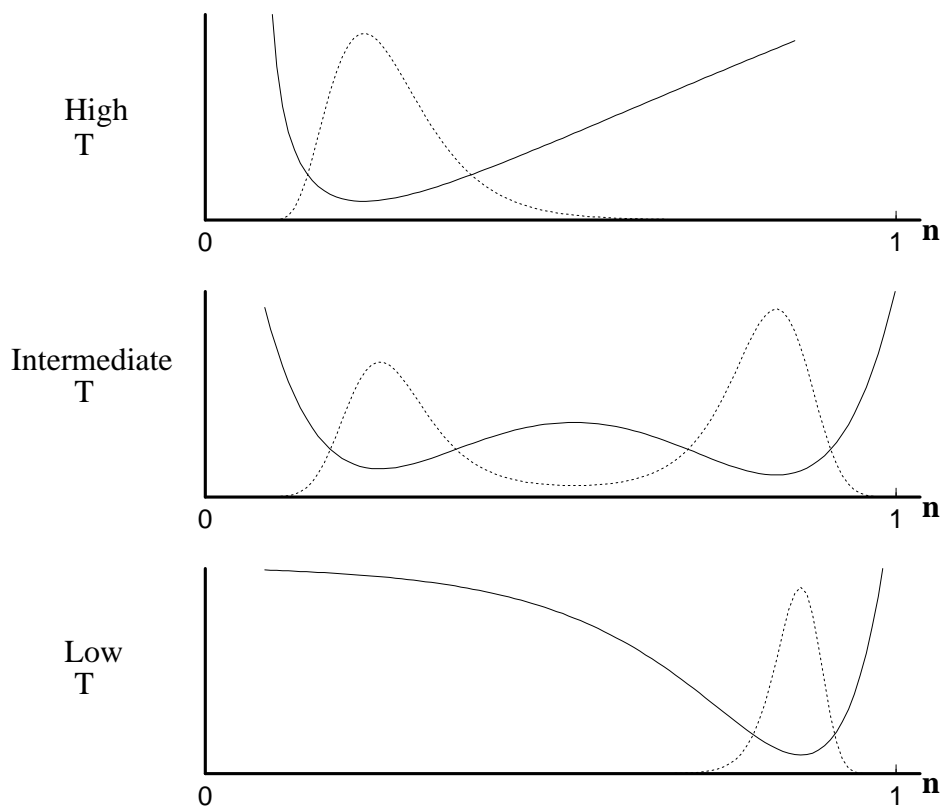
15

Figure 4: Sketches of the free energy (solid lines) and probability of occupation (dashed lines) against a folding reaction coordinate for three different temperatures. The value $n = 1$ corresponds to the native structure. The top sketch shows the situation for high temperatures, where the free energy function has a single minimum near $n = 0$, i.e., in highly unfolded states. Here the molecule is far more likely to be in an unfolded conformation than it is to be a conformation similar to the native structure, as it is shown by the dashed lines. As the temperature is lowered, the free energy develops a second minimum, one of them similar to native structure. There is a a free energy barrier between these minima. At these temperatures the probability of occupation is bimodal, with one unfolded and one nearly native peak. Finally at low temperatures, there is again a single minimum in the free energy, but this minimum is near the native structure. Here the molecule is very similar to the native structure.

in the molten globule phase and these can and should be taken into account in a complete analysis. However, the simple one-parameter analysis captures the essentials and should fit data over an appropriately restricted range of thermodynamic conditions.

IV   Quantitative Aspects of the Kinetics of a Folding Protein.

The theoretical formulation of the kinetics of protein folding differs from the classic formulation of transition state theory in some important ways. Most of our ideas concerning rate theory had their origin in studies of gas phase reactions of small molecules and simple unimolecular reactions in liquids [69, 70]. Four important properties of these simple reactions will illustrate the most important points of contrast with protein folding. First, in the simple reactions solvent is either absent or plays a passive role, *e.g.*, as a heat bath or source of friction. Second, the initial state, final state and transition state all refer to single, fairly well defined structures so entropy considerations are not important. Third, there is a single, fairly well defined reaction coordinate. Fourth, the effective diffusion coefficient for moving along the reaction coordinate changes very little as the system moves from the initial to the final state. Protein folding is completely different from these simple reactions [5, 40, 41, 71]. First, in protein folding, the solvent plays a vital role in stabilizing the folded state. As explained above, the important role of the solvent means that the potential of mean force, which here plays the role of the energy as a function of configuration, is a function of temperature and solvent conditions. Second, the initial denatured state, final folded state and transition states all refer to sets of protein structures, so the configurational entropy of the protein chain is a necessary part of the description of protein folding. Third, there are many possible reaction coordinates and pathways. Fourth, the dynamics of the protein chain changes qualitatively during the course of folding; in particular, an open chain, has far greater thermal motion than a collapsed chain. Therefore, the effective diffusion coefficient for motion along a reaction coordinate for folding probably can also change qualitatively between the initial and final states. Below we will discuss the modifications to the transition state theory framework that are needed to describe protein folding kinetics.

The gradient of the free energy function, $F(n)$, describes the overall tendency for the system to move and change its value of n. The average flow in configuration space will tend to minimize the free energy. For typical forms of the expressions for the energy and the entropy as a function of similarity to the native state, n, $F(n)$ will tend to have one or two minima, so the system will be unistable or bistable. If the system is unistable and the conditions are favorable for folding, then the single minimum of the free energy function must occur near the native state. A unistable free energy function with its minimum near the native state would require a huge thermal driving force. We call this situation "downhill" protein folding. Downhill folding is rare in slow timescale *in vitro* protein folding experiments carried out in conditions near the transition between equilibrium folding and equilibrium unfolding. Downhill folding may be common in strongly nativizing conditions, in the initial stages studied in fast timescale folding experiments [61] and *in vivo*. In downhill folding the protein folds by making a straight run down the average free energy gradient.

An analogy with transition state theory [69, 70] yields a simple estimate for the folding rate, or equivalently, the folding time [5]. In transition state theory the reaction rate is given

by the rate of going through the bottleneck for the reaction. Traditionally, this bottleneck is the highest free energy state in the reaction coordinate pathway from the reactant state to the product state. This bottleneck is called the transition state. In transition state theory the rate of going through the transition state depends on the free energy barrier, *i.e.*, the difference between the transition state free energy and the reactant state free energy. In downhill folding there is no free energy barrier. However, there is a bottleneck for folding in downhill folding, because the effective diffusion coefficient for motion along a reaction coordinate changes qualitatively during the course of folding; the region with the smallest diffusion coefficient is the kinetic folding bottleneck. Let $\bar{t}(n)$ denote the typical lifetime of an individual microstate with a similarity n to the native structure. This lifetime is a measure of the rate of motion along the reaction coordinates for folding; the larger $\bar{t}$ the smaller the effective diffusion coefficient and the slower the folding rate. The kinetic bottleneck for folding occurs at the value of n that maximizes $\bar{t}(n)$, which we denote by $n_{kin}^{\ddagger}$. The subscript *kin* stands for kinetic and the reason for using this subscript will become apparent below. Therefore, a simple estimate of the folding time, τ, in analogy with transition state theory, is given by

$$\tau = \bar{t}(n_{kin}^{\ddagger}). \qquad (9)$$

Notice that the time in equation (9) is a lower bound on the folding time, hence an upper bound on folding rate. This property is is expected because the transition state technique gives upper bounds on reaction rates [70]. We shall discuss the meaning of $n_{kin}^{\ddagger}$ in more detail below. For now notice that $n_{kin}^{\ddagger}$ is *not* the location of the top of the free energy barrier, as in conventional transition state theory.

The roughness of the energy surface determines the lifetime of individual microstates. The detailed distribution of these lifetimes can be determined from a detailed analysis and it is rather broad. However, a reasonable first approximation to the typical escape time is easy to obtain. Most minima along a perimeter of constant n are surrounded by ordinary states with nearly the average energy, $\bar{E}(n)$. Thus the barrier height for hopping is $\bar{E} - E_{m.p.} = (\Delta E / k_B T)^2$. This gives an escape time with a super-Arrhenius temperature dependence

$$\bar{t}(n) = t_0 e^{(\Delta E(n)/k_B T)^2} \qquad (10)$$

The prefactor t_0 is the timescale for a typical motion of a large segment of the chain. It depends on local barriers and on the solvent viscosity, which is itself temperature dependent. Isoviscosity studies of protein folding are therefore quite interesting. The non-Arrhenius temperature dependence exhibited here is sometimes called the Ferry law [72] and is describes the slow dynamics of many glassy systems. As expected, increasing the roughness of the energy landscape greatly slows down folding.

What happens to the escape process as the temperature is lowered? The above estimate assumes many channels for escape exist and an average one can be taken. But as the temperature is lowered it becomes preferable to find an unlikely channel with an improbably low barrier. A subtle analysis [5] shows that, for a given value of n, the escape time goes no lower than a "search" time

$$\bar{t} = t_0 e^{S_0(n)/k_B} \qquad (11)$$

This is the average number of steps taken by the protein to find a state of negligible barrier. This is the Levinthal time for searching states at fixed perimeters, i.e., fixed value of n. For a given n this escape time is reached at a temperature

$$T_g(n) = \left(\frac{\Delta E(n)^2}{2k_B S_0(n)} \right)^{1/2} \tag{12}$$

The analysis of Bryngelson and Wolynes also shows that for $T > T_g(n)$ the protein has kinetic access to representative section of the perimeter (see Fig. 2) so the behavior of a typical protein molecule can be replaced by the behavior of a statistical ensemble. In this case equations (9) and (10) for the folding time are valid.[3] For $T < T_g(n)$ the protein has kinetic access to very few structures. These structures are not necessarily representative of the statistical ensemble, so the proteins behavior is dominated by the details of its specific energy landscape. In this case equations (9) and (10) for the folding time must be modified. Technically, the kinetic behavior of the protein molecule becomes non-self-averaging, a term we discuss later in this section.

A system with a fixed n also undergoes a thermodynamic second order phase transition at $T_g(n)$ in which the protein is effectively frozen into one or few of a small number of low energy states. Using Eq. 6, we see that for $T \leq T_g(n)$, the number of thermally occupied states no longer scales exponentially with the size of the protein.[4] Conversely, as a protein folds at a fixed temperature T, the similarity to the native structure, n, becomes larger. However, the entropy, $S(E_{m.p.}(n), n)$, decreases as n becomes larger, i.e., there are fewer states available to the protein molecule as it approaches its native structure. A typical protein runs out of entropy at some value n_g of n. This vanishing of configurational entropy is precisely the previously noted second order phase transition, this time taking T rather than n to be constant. The critical values of the temperature and the fraction native structure are related by $T = T_g(n_g)$, where T is the temperature at which the folding experiment is carried out. In addition, Bryngelson and Wolynes have shown that the glass transition can only occur for a protein that already has collapsed [6]. Therefore, for any given temperature T, for values of $n \leq n_g(T)$ the kinetic description presented in this section is valid and the folding kinetics are self-averaging, and for $n > n_g(T)$ the protein is in the glassy phase, and its kinetics becomes non-self-averaging.

For bistable systems, there are two minima of free energy with a maximum of free energy between them. In folding conditions the minimum close to the native state has a lower free energy than the minimum corresponding to the unfolded state. The free energy barrier for folding, $F_{barrier}$, is given by the difference between the free energy of the unfolded minimum, $F(n_{uf})$ and the free energy of the the barrier top, $F(n_{th}^{\ddagger})$. The subscript th stands for thermodynamic and the reason for using it will become clear momentarily. Systems to the right of the top of the free energy barrier, i.e., with $n > n_{th}^{\ddagger}$, tend to become folded; those

---

[3]The more subtle analysis by Bryngelson and Wolynes shows that the full time dependence of $\bar{t}$ is slightly more complicated: For $T > 2T_g(n)$, $\bar{t}(n) = t_0 \exp[(\Delta E(n)/k_B T)^2]$, as in equation (10) above, but for $2T_g(n) > T > T_g(n)$, this equation must be modified to $\bar{t}(n) = t_0 \exp[S_0(n) + (1/k_B T_g(n) - 1/k_B T)^2 \Delta E(n)^2]$

[4]Applying equation 6 literally would imply a thermally accessible perimeter with less than one state because the entropy analysis neglects finite size corrections.

to the left, *i.e.*, with $n < n_{th}^{\ddagger}$, would become unfolded on the average. A straightforward generalization of transition state theory [5] indicates that the overall folding time is given by

$$\tau = \bar{t}(n_{kin}^{\ddagger}) e^{F_{kin}^{\ddagger}/k_B T} \tag{13}$$

where $F_{kin}^{\ddagger} = F(n_{kin}^{\ddagger}) - F(n_{uf})$ and $n_{kin}^{\ddagger}$ is the value of n that maximizes the above expression for τ. One may think of $n_{kin}^{\ddagger}$ as the similarity to the native state where the bottleneck for folding occurs. The set of states with $n = n_{kin}^{\ddagger}$ acts like the transition state for folding when we consider influences of external agents on rates.

Although equation (13) for the folding time has the same form as analogous expressions from traditional transition state theory, there are three important differences. First, the prefactor is $\bar{t}(n_{kin}^{\ddagger})$, the typical lifetime of an individual microstate at a similarity $n_{kin}^{\ddagger}$ to the native structure. The corresponding prefactor in absolute rate theory would be an expression only involving fundamental constants. The need for the prefactor based on the lifetime of the microstates stems from the greater complexity of protein folding as compared with the gas phase reactions which absolute rate theory was originally designed to describe. This lifetime strongly depends on the roughness of the surface. Ignoring this fact, we see that the folding is considerably less than the Levinthal estimate, because some of the configurational entropy loss is balanced by the gain in energy as the native structure is approached. The second difference is that $n_{kin}^{\ddagger}$, the analogue of the transition state in equation (13) for the folding time, is determined by maximizing the *entire* folding time expression in this equation. In contrast, in traditional transition state theory, the transition state is a maximum of the free energy, which would here correspond to $n_{th}^{\ddagger}$. If the average lifetimes $\bar{t}(n)$ were constant, *i.e.*, independent of n, then $n_{kin}^{\ddagger}$, would equal $n_{th}^{\ddagger}$. However, in protein folding, we expect the average lifetimes $\bar{t}(n)$ to vary strongly with n, so $n_{kin}^{\ddagger}$ will *not* always equal $n_{th}^{\ddagger}$ and the difference can be large and important. More concisely, the position of the *kinetic* folding bottleneck, $n_{kin}^{\ddagger}$, is not necessarily the same as the position of the *thermodynamic* folding bottleneck, $n_{th}^{\ddagger}$. Third, whereas in traditional transition state theory the transition state typically is a specific configuration, the transition state in our folding time expression (13) corresponds to an entire band of states in the full configuration space and should not be thought of as a unique configuration. Furthermore, since the potential of mean force of the protein chain is dependent on temperature and solvent conditions, the location of the transition state band will change as the temperature and solvent conditions change. This situation is in marked contrast to the case of small molecules in the gas phase in which the transition state can be thought of as a single structure which is fixed for all reaction conditions.

Notice that the free energy gradient provided by the minimal frustration principle leads to multiple paths approaching this transition state surface as long as the glass transition has not been reached and that this is crucial to overcoming the entropy loss on folding. The expected temperature dependence of the folding time is obtained by combining equation (13) for the folding time and equation (10) for the average lifetime of a microstate. The

20

result, after taking the logarithms in order to simplify the resultant expressions, is

$$\log\left(\frac{\tau}{t_0}\right) = \frac{F_{kin}^{\ddagger}}{k_B T} + \frac{\Delta E(n_{kin}^{\ddagger})^2}{(k_B T)^2} \tag{14}$$

Notice that if $F_{kin}^{\ddagger}$ and $\Delta E(n_{kin}^{\ddagger})$ are assumed to be temperature independent, then equation (14) implies that an Arrhenius plot of folding time versus inverse temperature would be curved, and in fact parabolic. Such curved Arrhenius plots are frequently observed in protein folding experiments [73]. Unfortunately, these plots can not be used to derive values for $F_{kin}^{\ddagger}$ and $\Delta E(n_{kin}^{\ddagger})$ directly. First, our discussion of microstate lifetimes is rather rough. A more careful treatment shows that the exponent in the expression for the lifetimes (10) must be replaced with a general quadratic in $\Delta E(n)/k_B T$ when the system gets close to the glass transition. Second, and more important, $F_{kin}^{\ddagger}$ *does* depend on temperature, because the free energies of the unfolded state and the folding bottleneck, the position of the folding bottleneck, the potential of mean force of the protein molecule all change with temperature. Similarly, $\Delta E(n_{kin}^{\ddagger})$ also depends on temperature. The main point here is that a curved Arrhenius plot of the folding time should be expected as an elementary consequence of energy landscape properties of protein folding.

The glass transition, discussed above for downhill folding, also occurs in systems with bistable free energy functions, in exactly the same way. As before, when the system $T > T_g(n)$ the behavior of a typical protein can be replaced by the behavior of a statistical ensemble, so equations (13) and (14) for the folding time are valid. For $T < T_g(n)$ the kinetics are dominated by the details of the energy landscape, so equations (13) and (14) for the folding time must be modified. The kinetic behavior in this glassy regime is non-self-averaging, a term we now discuss.

An important feature of protein folding below the glass transition is non-self-averaging behavior. The idea of non-self-averaging is best approached by first discussing its opposite, self-averaging behavior. In simple terms, a self-averaging property is one that depends on the overall composition of an object, rather than its detailed structure. An illustration of this idea is provided by alloys, for example, brass, an alloy of copper and zinc. No order determines whether a particular lattice site is occupied by a copper atom or a zinc atom, so each piece of brass is different on the atomic scale. However, in spite of these differences, all pieces of brass with sensibly the same composition share many properties, for example, hardness, density, electrical conductivity, *etc.*. These properties are called self-averaging because, the value of the property, say hardness, of member of a statistical ensemble, here pieces of brass with the same composition, is almost always nearly equal to the the average value of that property over the statistical ensemble.[5] Notice that self-averaging is a characteristic of the ensemble and the property taken together. Going back to the alloy example, density is a self-averaging property for all pieces of brass with a specified composition, but is not a self-averaging property for all pieces of metal. As a biochemical example, consider the

---

[5]More precisely, consider a statistical ensemble of objects, and some property of the objects in the ensemble. A property is called self-averaging if the fluctuations of the value of that property in the members of the statistical ensemble are small compared to the average value of the property over the ensemble. More detailed discussions of self-averaging can be found in the references on spin glasses that we cited.

ensemble of amino acid sequences with the same length and amino acid composition as hen lysozyme. The ability to form a collapsed globule with approximately the radius of gyration as a lysozyme molecule is probably a self-averaging property for this ensemble, whereas the ability to fold to a structure that hydrolyzes glycosidic bonds is almost certainly a non-self-averaging property.

The presence or absence of self-averaging of a given property has important practical implications. If a property is self-averaging over some ensemble, then studying that property in one member of the ensemble suffices to learn about the property for all members of the ensemble; if the property is non-self-averaging, then studying that property in one member of the ensemble provides no information about the property for other members of the ensemble. The question of whether or not a given property is self-averaging is also intimately related to the question of whether or not that property is strongly affected by mutations. A mutation will create a new sequence, *i.e.*, a new member of the ensemble. A self-averaging property will behave in the same way in the mutant as in the rest of the members of the ensemble, but a non-self-averaging property will behave differently in each member of the ensemble, including the mutant.

In protein folding there are several different ensembles over which one can average, a few of which we now list, going from the largest, most general ensemble to the smallest, most specific ensemble. First, there is the most general ensemble relevant to protein folding, that of all possible polymers of amino acids. Experiments on random polypeptide sequences explore this ensemble [35]. Next is the set of ensembles of amino acid sequences with fixed amino acid composition. Experiments that investigate random sequences with only a few types of amino acids have studied instances of these ensembles [36, 74]. Interestingly, there is some evidence from computer simulations of protein folding that the collapse time for a sequence depends only on its composition; this evidence indicates that collapse time may be a self-averaging property over these ensembles [90]. Finally, there are the ensembles of sequences that fold to a specific structure, *e.g.*, the different lysozyme sequences mentioned in the introduction. These ensembles are studied in research programs that investigate the properties of different mutants of a particular protein.

How do these considerations of the location of a second order phase transition corresponding to an ideal glass transition *along* the folding coordinate relative to the extrema of the unimodal and bimodal free energy functions affect the kinetics of folding? We see that there are several distinct folding scenarios, which are illustrated in Figure 5 and which we now discuss. As stated above, for a unimodal free energy function, downhill folding, the rate of folding will depend mainly on the lifetimes of the individual microstates. We call this situation a Type 0 scenario. It is analogous to spinodal crystallization studied in materials science [75]. In this case the unfolded state is unstable; from almost any configuration there is a conformational change that will lower the energy with little cost in entropy. Nevertheless, this type of folding transition can still have a folding bottleneck, like the folding transitions in a bimodal free energy function if the diffusion constant becomes small, as in a glass transition. The difference here is that the folding bottleneck in a Type 0 transition will be *entirely* kinetic, so $n_{kin}^{\ddagger}$ will occur at the maximum of $\overline{t}(n)$. In contrast, for a bimodal free energy function the folding barrier will have both kinetic *and* thermodynamic contributions. The Type 0 scenario can further be broken into two subclasses. In the first subclass,
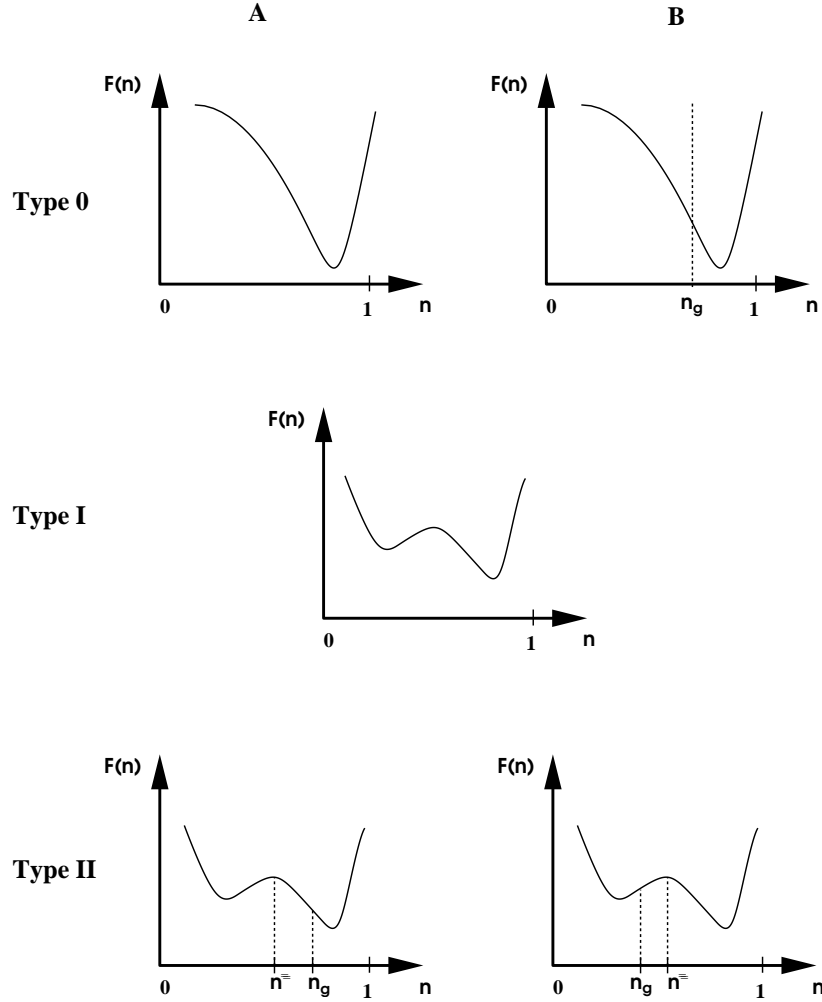
Figure 5: Schematic illustrations of the folding scenarios discussed in the text. Each sketch shows a qualitative plot of the free energy against the folding coordinate. In the type 0 scenarios shown at the top, the free energy function has only one minimum near the folded state, i.e., $n = 1$. In a type 0A transition, shown at the left, there is no glass transition. In a type 0B transition, shown at the right, at some value of the folding coordinate, n_g, the protein undergoes a glass transition and it exhibits the glassy dynamics described in the text for the remaining of the folding process, $n > n_g$. The type I scenario is shown in the middle of the figure. Here the free energy has two minima, an unfolded one and a folded one, and there is no glass transition during the folding process. The free energy functions in the type II scenarios, shown at the bottom of the figure, also have two minima but the protein undergoes a glass transition during the folding process. In a type IIA scenario, shown at the left , the glass transition occurs after the thermodynamic folding bottleneck at $n_{th}^{\ddagger}$. In a type IIB, shown at the right , $n_{th}^{\ddagger} > n_g$, making the folding protein glassy before the thermodynamic folding bottleneck is reached.

which we call Type 0A, the glass transition does not occur at any value of n. In this case the folding is fast and dominated by a single rate, the rate of going down the free energy gradient. The kinetics in this regime are self-averaging. In the second subclass, which we call Type 0B, the glass transition occurs before the protein reaches its native state. Then the first part of the folding is a rapid descent down the free energy gradient, as before, but the glass transition intervenes and slows the folding considerably. The overall kinetics is slower and multi-exponential because different protein molecules find themselves stuck in a few different microstates after the glass transition, and each of these states will fold at a different rate. Some of the microstate lifetimes can be very long. These long-lived microstates will be observable as kinetic intermediates. The paucity of occupied microstates will lead to discrete pathways as shown schematically in Figure 6. The kinetic behavior is strongly non-self-averaging, so mutations easily change the folding kinetics. Intermediates in one form of the protein are absent in others.

The kinetics of the folding of proteins with bimodal free energy functions fall broadly into two classes. In the first of these, which we call Type I, there is no glass transition at any point in the folding, just like the type 0A folding scenario noted above. Type I scenarios are analogous to nucleation followed by rapid growth [75]. In this case the folding is dominated by a single rate, the folding time being given by equation (13). The protein has kinetic access to a representative section of the folding bottleneck, so the rate of folding can be calculated by considering the rate of folding for a statistical ensemble of structures at the bottleneck. In this regime, the protein can take many possible pathways through the bottleneck, so the overall folding time will be independent of the initial unfolded configuration of the protein. The folding kinetics are self-averaging, so mutations will have only small effects on folding rates.[6] In the other class the glass transition occurs at some point in the folding process. We call these folding events Type II. Type II folding processes are analogous to nucleation followed by slow growth: a situation much studied in the metallurgy of alloys [75]. Type II folding scenarios can be broken into two subclasses, depending on where the glass transition occurs relative to the thermodynamic bottleneck location $n_{th}^{\ddagger}$. Recall that $n_{th}^{\ddagger}$ is the location of the maximum of the free energy and need not be the same as the kinetic bottleneck coordinate $n_{kin}^{\ddagger}$ that appears in equations (9) and (13) for the folding time. Thus, for folding at a fixed temperature in a situation where a glass transition occurs, we expect to find two distinct kinetic scenarios, one, which we call Type IIA, occurs when $n_{th}^{\ddagger} < n_g$, and the other, which we call Type IIB, occurs when $n_{th}^{\ddagger} \geq n_g$.

As the roughness of the energy landscape is increased, a glass transition occurs between the folding bottleneck and the final folded state, so that discrete pathways occur after the transition state. We call this situation a Type IIA scenario. In this regime passage through the folding bottleneck will be dominated by a single rate, but there may be some non-exponential behavior, and discrete pathways and kinetic intermediates will be observed in the late stages of folding.

---

[6]To be more precise, rates of individual events depend on the exponentials of free energies. Above the glass transition these free energies should all self-average and the significant rates will have a log-normal distribution. A few factors of two change in the rate is not considered significant here. In the glassy phase a much wider distribution of the logarithm of the rate is anticipated, as pointed out by Bryngelson and Wolynes [5]
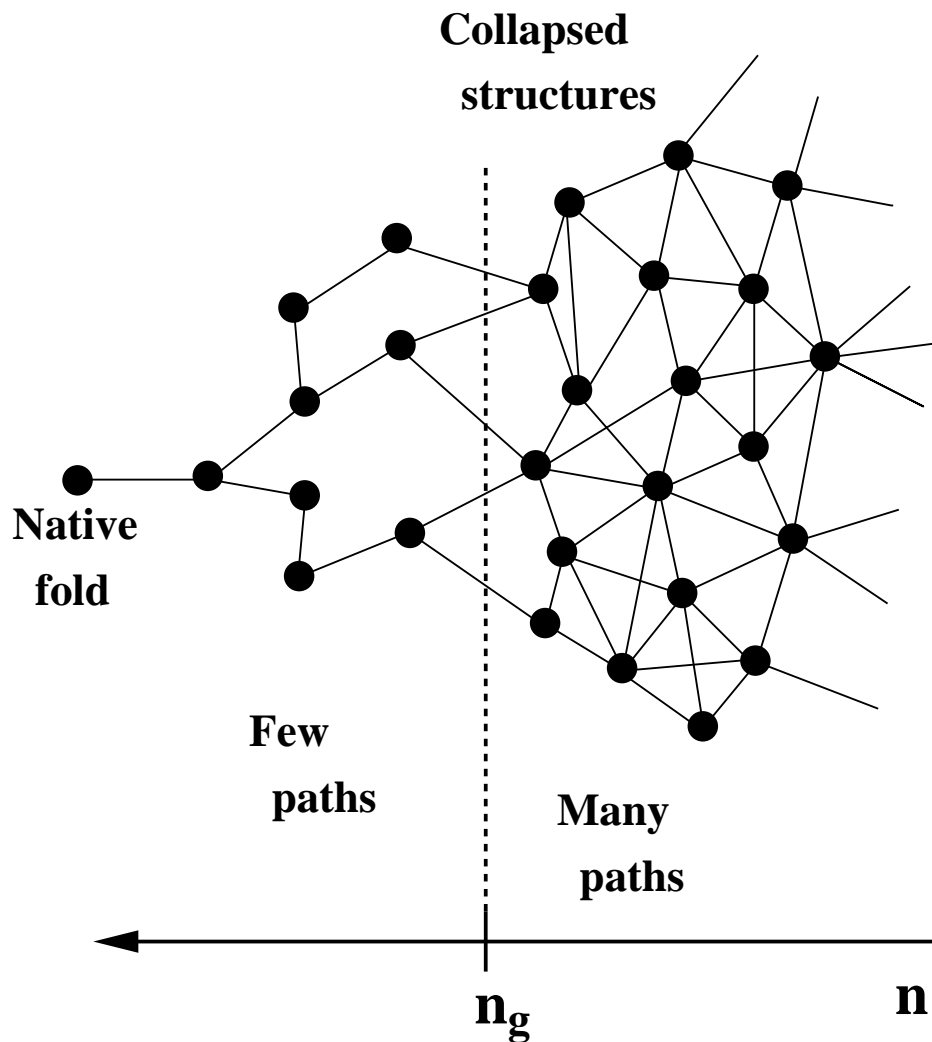
Figure 6: A schematic representation of the emergence of folding pathways. In this figure the native structure is on the left, so that n increases from right to left. Before the folding protein reaches the glass transition there are many accessible paths between conformations. In this regime each molecule would take a different path as it approached the native structure. After the folding protein goes through the glass transition it has access to only a few paths, so most molecules will take one of a few, or perhaps only one, path to the native structure.

In the Type IIB scenario the protein has already gone through the glass transition when it reaches the maximum of free energy. Since the protein can take only a few pathways after the glass transition, and these pathways can be different enough to lead to wildly different folding times, the overall folding time will strongly depend on which of the few paths to the folded state is taken. Each of these paths will have its own kinetic transition state and the free energies of these states will differ appreciably, *i.e.* they will not self-average. The importance, and even the meaningfulness, of the *typical* kinetic transition state, $n_{kin}^{\ddagger}$, is diminished considerably in this regime Therefore we have used the location of the glass transition relative to $n_{th}^{\ddagger}$ rather than $n_{kin}^{\ddagger}$ in defining the difference between the Type IIA and Type IIB scenarios.

V   The Phase Diagram and Protein Folding Scenarios.

The phase diagram is a powerful tool for understanding protein folding. It reduces much of the discussion about folding scenarios in the previous section to a single, clear, coherent picture which is useful for thinking about and planning experiments.

The simplified viewpoint of protein folding, using the energy landscape framework that we discussed in the last section can be used to classify different mechanisms of protein folding in the laboratory and in computer simulations. The analysis discussed above uses only a single parameter, n, to characterize the difference between the native structure and the unfolded structures. In fact, native proteins differ from unfolded ones in several ways, so this requires the introduction of several different similarity measures in thinking about folding processes. It is important, however, that the number of additional parameters is relatively small, thus giving a reduced description of the folding process. Indeed, many of the discussions of folding pathways have concentrated on these additional similarity measures or order parameters. Thus in many pictures of protein folding, *e.g.*, the framework model [76], one gives considerable emphasis to the initial formation of secondary structures. In other scenarios, the collapse and formation of secondary structures are considered to be separate events [6]. Additionally, proteins may consist of subdomains for which we may discuss the tertiary structure formation separately. This is particularly important in hierarchical pictures of protein folding [77]. With each of these similarity measures we can ask the way in which the formation of order is related to the roughness of the energy landscape and whether the transition occurs through many pathways or through a small number of distinct pathways. It is helpful to consider a phase diagram like the one illustrated in Figure 7.

In this phase diagram, we plot the possible equilibrium states of a protein as a function of temperature and roughness of energy landscape. The phase diagram contains a region of random coil, a collapsed phase, folded region with transition lines between these places, as well as a dotted line indicating the presence of frozen glassy state.

A given protein will exist at equilibrium somewhere in this phase diagram, thus the diagram tells us the final state which we would obtain in an experiment. The folding process begins by starting in a configuration characterized by one of the regions on this diagram, but is carried out at a temperature such that the folded protein is the lowest free energy state. The roughness of the energy landscapes is important in determining the equilibrium phase but plays a bigger role in the kinetics of the folding process as described before. In
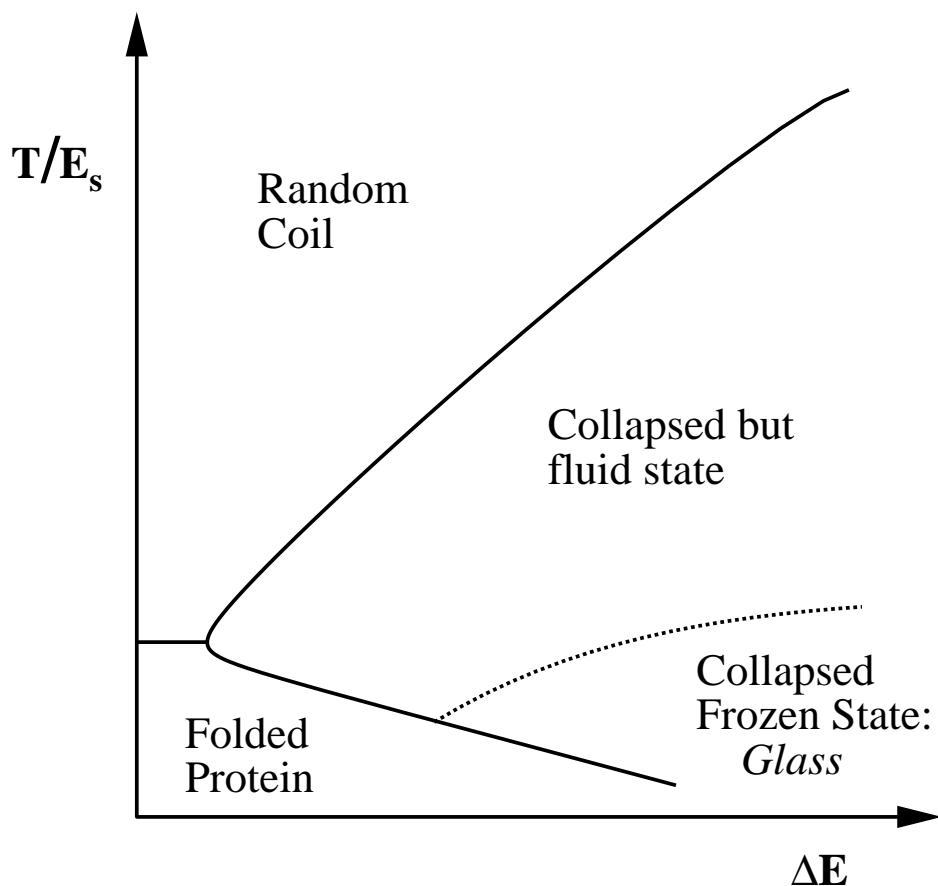
26

Figure 7: Phase diagram for a folding protein. The horizontal axis is the energy landscape roughness parameter, ΔE, discussed in the text. The vertical axis is the temperature divided by the stability gap E_s. The stability gap is the energy gap between the set of states with substantial structural similarity to the native state and the lowest of the states with little structural similarity to the native state. The collapse transition and the (first-order) folding transition are represented by solid lines and the (second order) glass transition is represented by a dashed line. In comparing this phase diagram with experimental phase diagrams, one must bear in mind that both ΔE and E_s are temperature dependent because of the hydrophobic force. In addition, the collapse transition depends on the average strength of the hydrophobic force, and this is both temperature and pressure dependent. The average strength of the hydrophobic force could be considered as a third dimension in the phase diagram.

the lefthand part of the diagram, folding will occur by a Type I mechanism in which discrete pathways are not observed. As the roughness is increased, the folding can occur by a Type IIA mechanism in which discrete pathways occur after the transition state. As the roughness of the energy landscape increases more, and the equilibrium glass transition occurs before the transition state is reached so the folding occurs through a Type IIB mechanism in which discrete pathways are observed and misfolded states play a role in the dynamics. Structurally unique thermodynamic transition states (bottlenecks) can occur only if $T < T(n_{th}^{\ddagger})$, *i.e.*, if the folding is Type IIB, because that is the only case where there are order one accessible paths through the folding bottleneck. In all other folding scenarios, there are many accessible paths through the folding bottleneck, hence many possible transition states.

The temperature at which the folding experiment takes place also plays an important role in whether a Type 0, Type I or Type II scenario for folding is observed. At low temperatures, (relative to the roughness energy scale) one expects to see nonexponential kinetics characterizing a Type IIB scenario. On the other hand, at higher temperature, at the midpoint of the folding transition, one expects to see Type I or IIA mechanisms to be more prevalent. Since ruggedness only appears when contacts are made, when there is little frustration, as well as little average driving force towards hydrophobic collapse, a Type I mechanism is most probable. This is very close to the framework model [76] or diffusion collision-picture [78–82] that was so often thought to describe protein folding. In the original versions of such models, only correct structures are formed initially and these can dock to form completed structures. Such a highly unfrustrated situation seems to be uncommon and certainly does not occur in the computer simulations of protein-like models.

Good folding sequences are ones that have a strong free energy gradient leading to the ground state structure. To achieve this they must separate in energy the native conformation and those conformations that are structurally similar to the native conformation from the bulk of most of the other conformations with no structural similarity to the native conformation. Goldstein, Luthey-Schulten and Wolynes have shown that this qualitative criterion is equivalent to finding sequences that maximize T_f/T_g for a suitable simplification of the Bryngelson-Wolynes model [83]. Notice that the energy gap that is being maximized when T_f/T_g is maximized is *not* the energy gap between any two specific states, but rather the gap between the *set* of states with substantial structural similarity to the native state and the lowest of the *set* of states with little structural similarity to the native state. We call this gap the "stability gap" (E_s). The stability gap should not be confused with the energy gap between the native configuration and the configuration with the next highest energy. This state will usually be native-like itself. There are too many fluctuations in the folded state for this two-configuration energy gap to have any significance for protein folding or stability [17, 18, 58, 85]. In fact, Frauenfelder and collaborators have interpreted the results of their experiments on *folded* proteins in terms of a hierarchy of "substates". These substates correspond to slightly different structures found in the population of folded proteins [18]. Evidence for the highest level of this hierarchy has been seen in protein folding simulations [59]. Unfortunately, this issue of energy gaps has been clouded by lattice simulations that have studied the energy spectrum of only the maximally compact states [71, 86]. Since the maximally compact states are a small fraction of all possible states and since the they are often not dynamically connected, (in the sense described in Section 2) [15, 40] the

interpretation of the results of these simulations requires more subtlety than has been found in the literature so far. Notice, however, that since local excitations from a maximally compact state are not themselves maximally compact, the energy gap between the native state and the next lowest energy maximally compact state is often correlated with the stability gap. Thus, the results of these simulations can be interpreted as a confirmation of the older and more general idea the sequences with large stability gaps fold quickly at the equilibrium folding temperature [4–6, 83, 84].

In the Bryngelson-Wolynes energy landscape the stability gap is a tautological consequence of the greater degree of stability of native-like interactions demanded by the principle of minimal frustration. Goldstein, Luthey-Schulten and Wolynes calculated a set of parameters that maximized T_f/T_g for the model used in their protein structure prediction algorithm, and found that these parameters gave excellent results for practical structure prediction, in accord with the predictions of the theory. In addition, molecular dynamics calculations using associative memory Hamiltonians optimized in this way reliably gave native-like structures [83, 84]. These results provide independent evidence that sequences that satisfy this criterion (of having a large stability gap) should be good folding sequences. This work also is a good illustration of the power of using energy landscape ideas to help solve practical protein folding problems. We also mention that the stability gap idea has been used by by Wodak and co-workers to predict persistent secondary structures in small peptides relevant to early folding events [87].

The phase diagram, of course, becomes more complex as additional order parameters or similarity measures are used to characterize the folded states. The phase diagram is a useful way of thinking about any folding process because it allows us to consider the couplings between the various order parameters as well. For instance, as one sees in the computer simulations one can first have a collapse which is ascribed by a single-order parameter radius of gyration, followed later from this collapsed phase by a transition to a unique folded protein structure [40, 88–90]. The coupling between these two parameters is crucial in obtaining that sort of description. The so-called molten globule intermediates which are often an ensemble of individual configurations really should be described by these additional order parameters [68].

VI   Energy Landscape Analysis of Folding Simulations

Simulations of simple protein-like lattice models provide an ideal ground to illustrate the energy landscape ideas. Lattice models have a venerable history [50–52, 91–100]. There is widespread agreement that they capture some of the underlying physics of protein folding. There are also excellent reviews that discuss lattice simulations in the context of the general problem of understanding protein folding [63, 101, 102]. Many groups have interpreted their simulation results using some of the qualitative and semi-quantitative ideas of energy landscape analysis, finding features in agreement with the overall picture that we have just discussed [40–42, 58, 59, 71, 103, 104]. Here we illustrate this kind of discussion by focusing on some recent results of Socci and Onuchic which find evidence for specific features arising from energy landscape analysis [90]. In addition, these simulations provide an excellent example of the kind of quantitative analysis which should be carried out for real experimental

Run	Sequence	E_{min}	τ_{min}	T_g	T_f
002	ABABBBBBABBABABABAAABBAAAAAAB	-84	2.0×10^7	1.00	1.285(15)
004	AABAABAABBABAAABABBABABABBB	-84	1.6×10^7	0.96	1.26(1)
005	AABAABAABBABBAABABBABABABBB	-82	2.3×10^7	0.98	1.15(2)
006	AABABBABAABBABAAABABAABBBB	-80	5.2×10^7	1.07	0.95(6)
007	ABBABBABABABAABABABABBBABAA	-80	9.3×10^7	1.09	0.93(5)
013	ABBBABBABAABBBAAABBABAABABA	-76	9.7×10^7	1.01	0.83(5)

Table 1: The various sequences used in this paper. The last four (005, 006, 007, 013) were generated at random. Sequence 002 is from reference 124. Sequence 004 is a single monomer mutation of 005 ($B_{13} \to A$). Both 002 and 004 have the lowest energies possible for the potential used and have native states that are completely unfrustrated, i.e. every native contact is individually stabilizing. τ_{min} is the fastest folding time for each sequence. T_g is the glass transition temperature (calculated with a $\tau_{\mathrm{max}} = 1.08 \times 10^9$). T_f is the folding temperature calculated using the Monte Carlo histogram method. The numbers in parenthesis indicate the uncertainty of the last digit.

data. We will use simplified quantitative relations that can be deduced from the energy landscape analysis. This sort of quantitative analysis should also be carried out for laboratory experiments, but in the laboratory the temperature dependence of the various free energy contributions must also be included explicitly for a fully convincing analysis. Simulations based on reduced models avoid these issues since the energy function is itself not temperature dependent.

The simulations were performed on polymers that were 27 monomers long which have maximally compact states of 3×3×3 cubes. Because the configurations on the 3×3×3 cube can be completely enumerated in a reasonable amount of computer time, the energy landscape among the maximally compact states can be explored in great detail. This 27 monomer cubic simulation has been a paradigm of study in this field because of this feature [54, 55, 71, 86, 105]. The simulations of Socci and Onuchic contain two monomer types. Pairs of monomers that were nearest-neighbors on the lattice but not connected along the chain contributed an interaction energy to the potential. The potential for the two monomer code was is -3 for contacts between monomers of the same type and -1 for contacts between different types. The folded configuration was taken to be maximally compact configuration with the lowest energy.

The characteristic energy scales and temperatures for different sequences is easily obtained for these models. The folding temperature, T_f, may be defined in the usual way as the temperature at which population in the folded configuration is equal to the populations in all other configurations. These populations can be obtained by a Monte Carlo sampling procedure for each of the sequences. The folding temperatures correlate rather well with the energy of the folded configuration. This is shown in Table 1. Figure 8 shows the equilibrium folding curves for these sequences.

A kinetic glass transition temperature can be defined without appealing explicitly to the energy landscape analysis. Just as in a laboratory, a kinetic glass transition temperature is defined by asking where a characteristic timescale in the problem exceeds some large value. In the simulations the maximum running time was $\tau_{\mathrm{max}} = 1.08 \times 10^9$ Monte Carlo steps. This number was chosen because it was significantly longer than the folding times over a broad range of temperatures. It would be appropriate to define the characteristic time through the
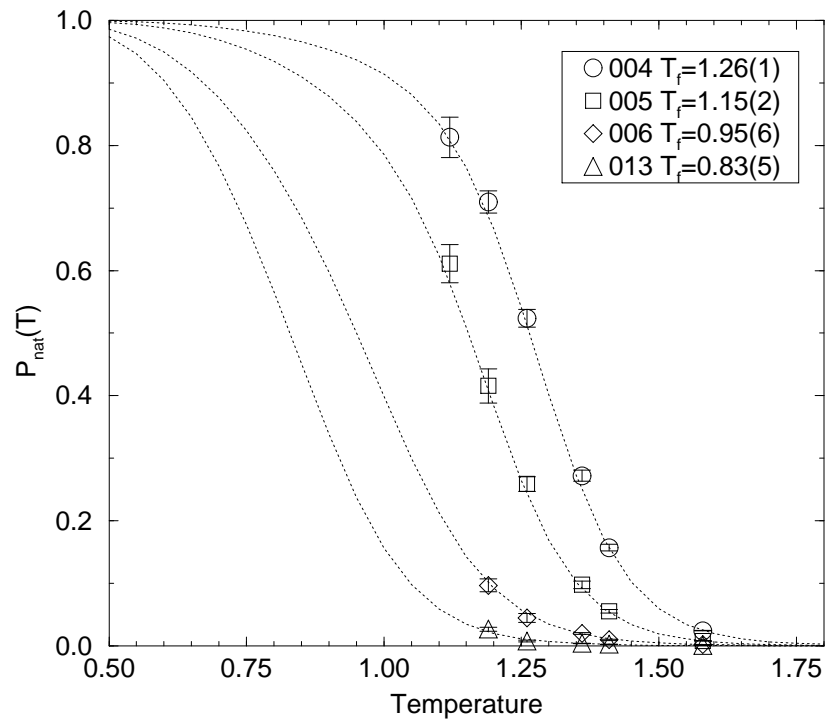
Figure 8: Folding curves for four of the sequences used in the simulation. The probability of a sequence occupying the native structure is plotted on the vertical axis versus temperature on the horizontal axis. The folding temperature, T_f, is defined as the temperature where $P_{nat}(T_f) = 0.5$, i.e., the probability of the occupancy of the native structure is one-half. The numbers in parenthesis indicate the uncertainty in the last digit.

typical time for a large-scale rearrangement. However, it is simpler here to use the folding time itself as a time-scale. A kinetic glass transition temperature, T_g, then is defined by the criterion $\tau_f(T_g)$ is $(\tau_{\max} + \tau_{\min})/2$ where $\tau_f(T)$ is the folding time at temperature T. As you can see from Table 1, this transition is nearly self-averaging, that is, it depends very little on the particular sequence which is studied, and is roughly 1.0.

According to the energy landscape analysis this kinetic glass transition is most strongly influenced by the thermodynamic glass transition. The simulations bear out this expectation. Changing the fiducial cut-off time by a factor of 8 causes only a 10 percent change in the kinetic T_g. Similarly, small changes to the algorithm for selecting the moves have a small effect on T_g.[7]

The thermodynamic glass transition of the BW analysis depends on the entropy and roughness energy scale of the compact states. This thermodynamic T_g is also a self-averaging quantity. Using only the maximally compact cube states, one obtains $T_g \approx 1.17$. This estimate of T_g is likely an upper bound, since semi-compact states also contribute to the entropy. At the same time, kinetic constraints could create additional restrictions on this connectivity. These effects seem to cancel, so the kinetic and thermodynamic glass transitions are rather close and one can take them both to be approximately 1 in analyzing the figures.

Figure 9 shows a plot of the folding time, that is, the time that takes for a random unfolded initial condition to reach the native structure, for different temperatures.[8] Since the 27 monomer length heteropolymer is so small, it is possible to analyze folding both above and below T_f for quite a range of temperatures. Above T_g the folding process is essentially an uphill one but with a modest slope. The first noticeable feature about the folding data is that they are strongly sequence dependent at intermediate temperatures. In the simulations, and folding times greater than a maximum of $\tau_{\max}$ were assigned the folding time $\tau_{\max}$. This is the origin of the saturation at the high and low temperature ends of these curves. At high temperature the folding is slow because it is so strongly uphill entropically. At low temperatures the folding is slow because of the roughness of the energy landscapes for all of these sequences. Another characteristic feature, however, is that the folding time at intermediate temperatures is most strongly correlated with the stability of the folded state for each of the sequences. The fastest folding sequence has the highest folding temperature, while the slowest has the lowest folding temperature. Indeed, the slowest folding sequence has a folding temperature less than the glass transition temperature.

Also plotted in Figure 9 are two different collapse times for the same sequences. The lower curve is the time that it takes the sequence to encounter, for the first time, a structure with 25 contacts. The middle curve is the time needed by the protein to achieve any maximally compact 28 contact cube. The remarkable qualitative feature of these collapse time curves is that at the moderate to high temperatures where the folding times vary greatly, all of the sequences have essentially the same collapse times. In this temperature range collapse is a self-averaging process that depends primarily on the average composition of the protein molecules. Another remarkable feature, however, is that the collapse time begin to

---

[7]Only if the number of crankshaft moves is reduced to less than 10 percent of the corner moves is there any very dramatic change in T_g.

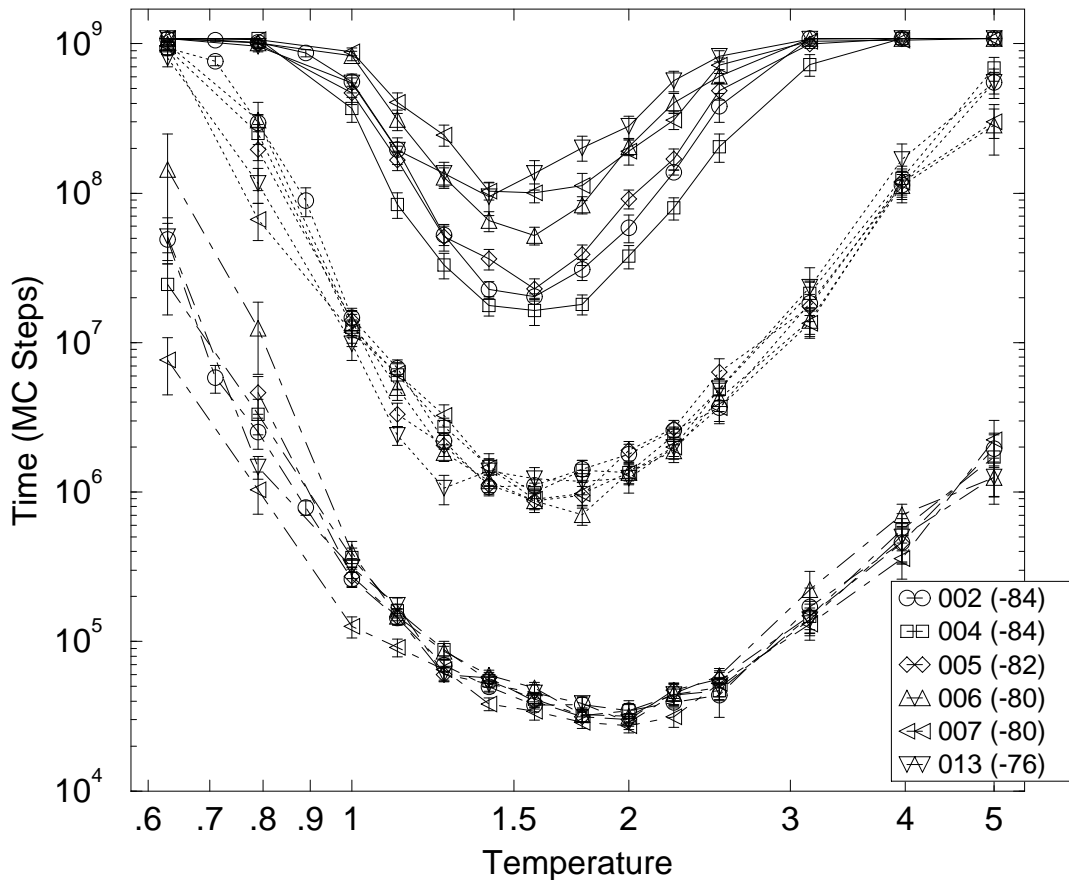[8]Technically, these times are mean-first-passage-times.

Figure 9: Plots of important times (in Monte Carlo steps) against temperature for the sequences used in our simulations. The top curves are the folding times τ_f (the number of steps required to reach the native structure for the first time). The saturation at the wings of the curves occurs because runs were stopped at a maximum time of 1.08×10^9 Monte Carlos steps. The other curves are plots of collapse times. The middle curves are the times required for the sequences to reach a conformation with 28 contacts for the first time. Similarly, the bottom curve is the time required to reach a conformation with 25 contacts for the first time. Notice that there is a much greater time spread in the folding curves than in the two collapse curves.

fluctuate greatly between different sequences at and below the kinetic glass transition temperature. The energy landscape analysis suggests that individual transition times between states fluctuate greatly below T_g, and this is reflected in the collapse process. The distribution of folding times becomes broader as you approach T_g, reflecting the emergence of a multi-exponential collapse process. We note that Flanagan *et al.* have observed sequence dependent collapse in staphylococcal nuclease [106]. This suggests the phase observed is near its glass transition.

A rough quantitative understanding of these data for folding and collapse comes from energy landscape analysis. The availability of both folding and collapse results allows us to roughly separate features connected with the glassy dynamics from the thermodynamic changes that also result from rough energy landscapes. The first important observation is that both folding and collapse times give parabolic Arrhenius plots, just as most experimental data do for the forward and reverse rate of folding [73]. In the laboratory this curvature is usually ascribed to the thermodynamic dependence of the effective interactions, the difference of heat capacity between the folded and unfolded states arising from the hydrophobic effect. Since the force laws in the simulation are taken to be *independent* of temperature, the temperature dependence of the hydrophobic effect is not at all involved in the simulation data. The simulation of Miller *et al.* also effectively finds a curved Arrhenius plot [107]. A simple analysis can be carried out by assuming that the location of the folding bottleneck, $n_{kin}^{\ddagger}$, is independent of temperature. Roughly speaking then, the folding time will be given by equation (13) with the energy barrier $F_{kin}^{\ddagger}$ given by the difference in free energy between the folding bottleneck states and the free energy of the bottom of the unfolded free energy minimum, *i.e.*, the lowest free energy unfolded states. This involves motion on the free energy gradient for the reaction coordinate based on the number of correct contacts. At this level of analysis, the collapse time can be treated in a similar way using the total number of contacts of any kind as a reaction coordinate. In the temperature range of 1.0 to 2.25 (the reason for considering this temperature range will become clear below) the time required for collapse to configurations with 25 contacts varys by a factor of less than 4, indicating that there is little, if any, free energy barrier to collapse. Therefore, collapse is essentially downhill in free energy and behaves like a Type 0A scenario. The dynamical reorganization timescale will become longer as the protein becomes more compact because excluded volume has a stronger effect on dynamics in compact states. Therefore, in the generalized transition state approximation of Section 4, the collapse time will be given by equation (9) for the time for a downhill process,

$$\tau_{collapse} = \overline{t}_{collapse}, \tag{15}$$

where $\overline{t}_{collapse}$ is the typical lifetime of an individual microstate in a random collapsed state. For the purposes of calculating the barrier height, $F_{kin}^{\ddagger}$, we set the free energy of the bottom of the unfolded free energy minimum equal to the free energy of the collapsed states. Then the folding time involves the free energy difference of the folded and compact configurations. Another way of obtaining a folding time that depends on this free energy difference is to consider folding to be a three state unimolecular reaction, *random coil* $\rightleftharpoons$ *collapsed* $\rightarrow$ *folded*, where the second step, *collapsed* $\rightarrow$ *folded* is rate-limiting. The data is consistent with such a reaction scheme.

We can eliminate the purely dynamical factors by taking the ratio of the folding to the

Run	A $= S_0(n^{\ddagger}_{kin}) - S_{0,collapse}$	B $= \overline{E}(n^{\ddagger}_{kin}) - \overline{E}_{collapse}$	C $= (1/2)[\Delta E(n^{\ddagger}_{kin})^2 - \Delta E^2_{collapse}]$
002	19.0	-34.9	23.8
004	17.0	-30.1	20.1
006	16.9	-25.2	16.1
007	16.1	-22.2	15.0

Table 2: The coefficients of the parabolic fits, $\log(\tau/\tau_{collapse}) = A + B/T + C/T^2$, to the data shown in Figure 9. The sequence numbers refer to the sequences displayed in Table 1. The column headings also show the physical chemical interpretations of the coefficients given in equation (16) in the text.

collapse time and assuming that $\overline{t}(n^{\ddagger}_{kin}) \approx \overline{t}_{collapse}$. Then using the equation (13) for the folding and collapse times and using equation (8) for the free energy predicts that a plot of the logarithm of the ratio of the folding to the collapse times to be parabolic,

$$
\log\left(\frac{\tau}{\tau_{collapse}}\right) = \; - \; [S_0(n^{\ddagger}_{kin}) - S_{0,collapse}]
$$
$$
+ \; \frac{[\overline{E}(n^{\ddagger}_{kin}) - \overline{E}_{collapse}]}{k_B T}
$$
$$
- \; \frac{[\Delta E(n^{\ddagger}_{kin})^2 - \Delta E^2_{collapse}]}{2(k_B T)^2}, \tag{16}
$$

where the subscript *collapse* indicates that the quantity is evaluated in a random collapsed state. The log of this ratio is plotted *versus* $1/T$ in Figure 10. We show here the data only between temperatures 1.0 and 2.25 because outside this range the folding times exceed the time used as a cut-off in the simulations. These curves can be fit very adequately with parabolas. The coefficients of the parabolas are shown in Table 2. In the fit all of the constant terms are positive and all of the linear (in $1/T$) terms are negative, which imply the inequalities $S_0(n^{\ddagger}_{kin}) < S_{0,collapse}$ and $\overline{E}(n^{\ddagger}_{kin}) < \overline{E}_{collapse}$. Both of these inequalities are consistent with the bottleneck for folding occurring after the collapse, in agreement with both intuition and the simulation data. The curvature reflects the value of the roughness of the energy landscape of the collapsed configurations. This analysis shows that for a rough energy landscape, the heat capacity of the collapsed configurations arises from fluctuations in structure and corresponding energy differences between collapsed configurations. The linear term in $1/T$ reflects primarily the enthalpic part of the activation free energy for achieving a transition state. It should be strongly correlated with the stability gap.

One can also check the theory by using independently derived information about the simulation model to make order-of-magnitude estimates of the sizes of the coefficients in the parabola fits. The constant term is the difference of the configurational entropies of the collapsed states and the folding transition bottleneck states. The number of states with 25 contacts has been estimated to be 10^9, yielding a configurational entropy of $9 \log 10 \approx 21$. The configurational entropy of the folding bottleneck states is more difficult to estimate, but it is clearly less than that of the collapsed states. Therefore, the constant coefficient is expected to be of order 10, i.e., between ≈ 3 and ≈ 30. This expectation is very well confirmed by Table 2, where the constant coefficients are see to lie between 16 and 19.
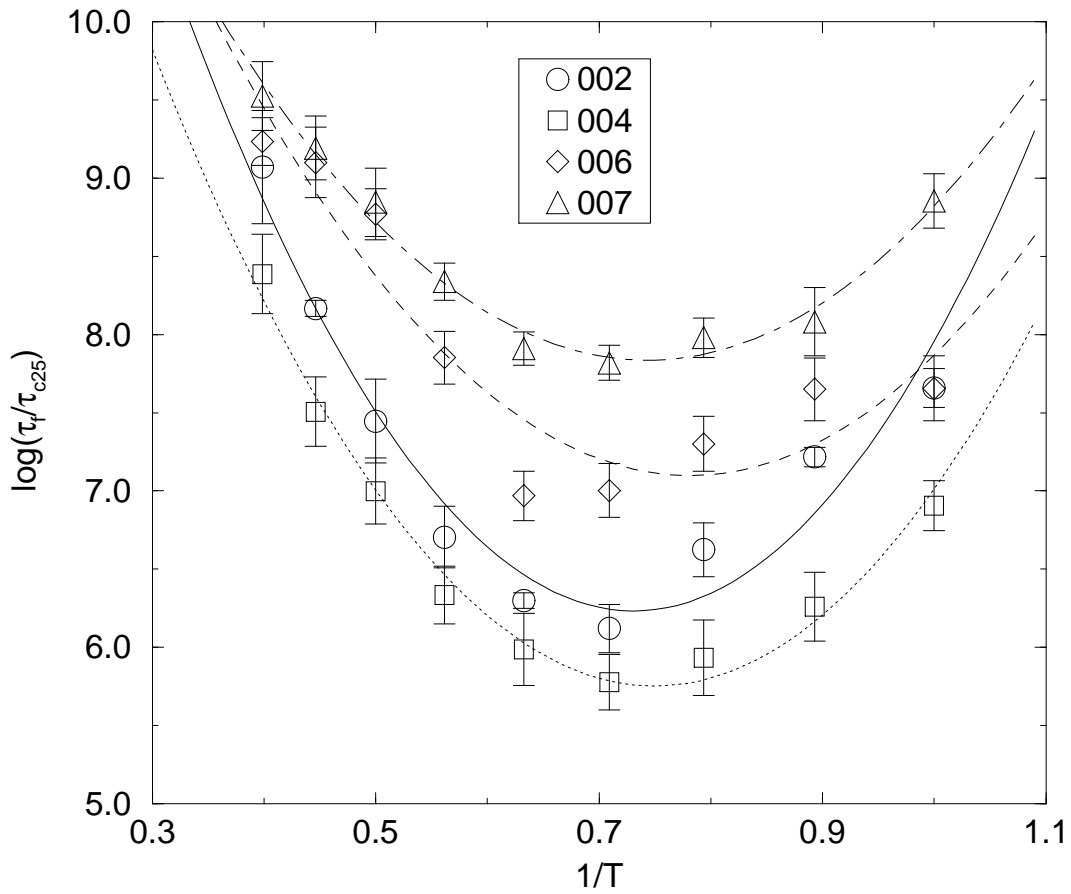
Figure 10: The logarithm of the ratio of the folding time to the time for collapse to 25 contacts against the inverse temperature. The lines are parabola fits to the data. The coefficients of these parabolas are shown in Table 2.

The coefficient of the $1/T$ term is the difference between the average energy of the folding bottleneck states and the collapsed states. We have defined a collapsed state to be a state with 25 contact and the average contact energy in our model is -2, therefore, the average energy of a collapsed state is -50. The average energy of a folding bottleneck state must be greater than the energy of the native state, which is -84 for sequences 002 and 004 and -80 for sequences 006 and 007. (See Table 1). Therefore, we expect the coefficient of the $1/T$ term to lie between 0 and -34 for the first two sequences and to lie between 0 and -30 for the later two sequences. Table 2 shows the coefficients to lie within these bounds, within reasonable error estimates. The coefficient of the $1/T^2$ term is one-half times the difference between the roughnesses of the the collapsed states and the bottleneck states. Each interaction energy in the model differs from the average interaction energy by $+1$ or -1, so the roughness of the set of random collapsed states with 25 contacts is $\Delta E = 25$. The roughness of the bottleneck states is smaller than this number, but difficult to estimate. Thus, we expect the coefficient of the $1/T^2$ term to be somewhat less than 12.5. The values for this coefficient range from 14 to 24, as shown in Table 2. This estimate is not as good as the previous ones, but it does give the right sign and order-of-magnitude, which is the best that can be expected from such an approximate theory and such simple estimates.

A quantitative relationship between protein folding kinetics and the thermodynamic stability of the native state can be obtained with linear free energy relationships [70, 108–110]. In the past these relations have been applied to the interpretation of data from site-directed mutagenesis experiments [111–114]. They are also the mainstay of the analysis of many other biochemical reactions [115–117]. In this analysis the differences in the free energies of the transition states, folded states and unfolded states for two different sequences are obey the linear relation

$$\delta F(n_{kin}^{\ddagger}) = \alpha \delta F(1) - (1 - \alpha)\delta F(0). \tag{17}$$

The transfer coefficient α is a measure of the resemblance of the transition state to the folded state. The value of α is easily obtained from the data. If we make the obvious assumption that the dynamical factors are approximately the same for the different sequences, then equation (17) implies that a plot of the logarithm of the folding rate against the logarithm of the equilibrium constant for folding will be a straight line with a slope of α [118]. When we plot the logarithm of the folding rate *versus* the logarithm of the equilibrium constant for different sequences, we see such a nice linear free energy relationship, shown in Figure 11. At the temperature $T = 1.0$ the folding time seems nearly independent of the driving force, while the driving force is entirely reflected in the unfolding rate. Thus folding here is nearly entirely "downhill", a Type 0 scenario. (The large fluctuations suggest a Type 0B.) At $T = 1.26$ there is a clear nucleation barrier, but it is small. The transfer coefficient of $\alpha = 0.1$ suggests a rather early transition state, *i.e.*, at this temperature the bottleneck configurations are collapsed but have little native structure. The further increase of α at higher T reflects a later transition state as the entropy terms become more important. This shows that the transitions are only weakly Type I and essentially Type 0 under these thermodynamic conditions. The success of this analysis is remarkable because the native structures corresponding with the sequences are not strongly related to each other unlike the situation in site-directed mutagenesis experiments.

An Arrhenius plot of the unfolding time *versus* $1/T$ is shown in Figure 12. This curve
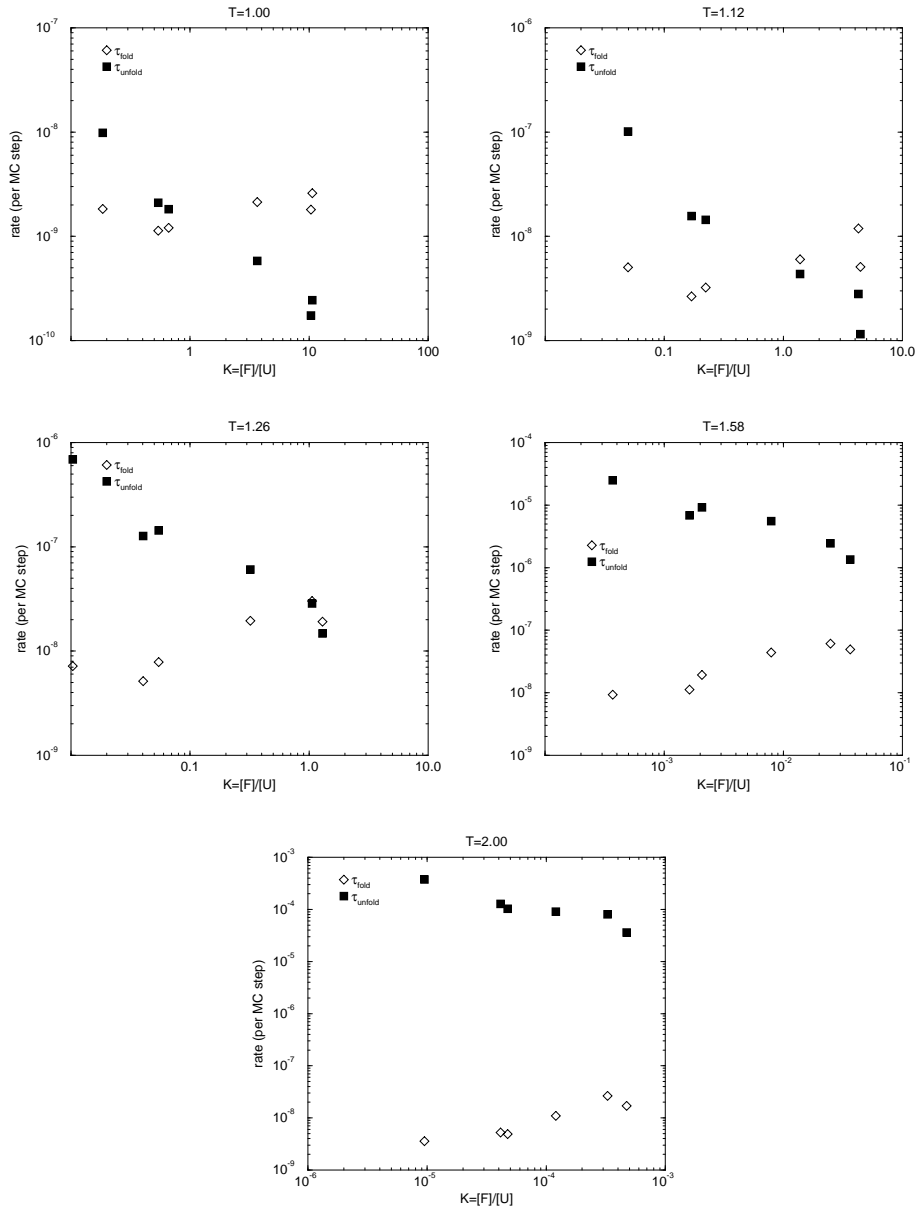
Figure 11: Plots for the linear free energy relationship analysis. Each plot shows the folding rate against the folding equilibrium constant for each of the six sequences studied here. On the horizontal axis $[F]$ represents the probability of the native structure being occupied and $[U]$ represents the probability of a non-native structure being occupied. Figure 11a is such a linear free energy plot for temperature $T = 1.0$, that is, at about the glass transition temperature for these sequences. The rest of the plots are for temperatures above the glass transition temperatures.
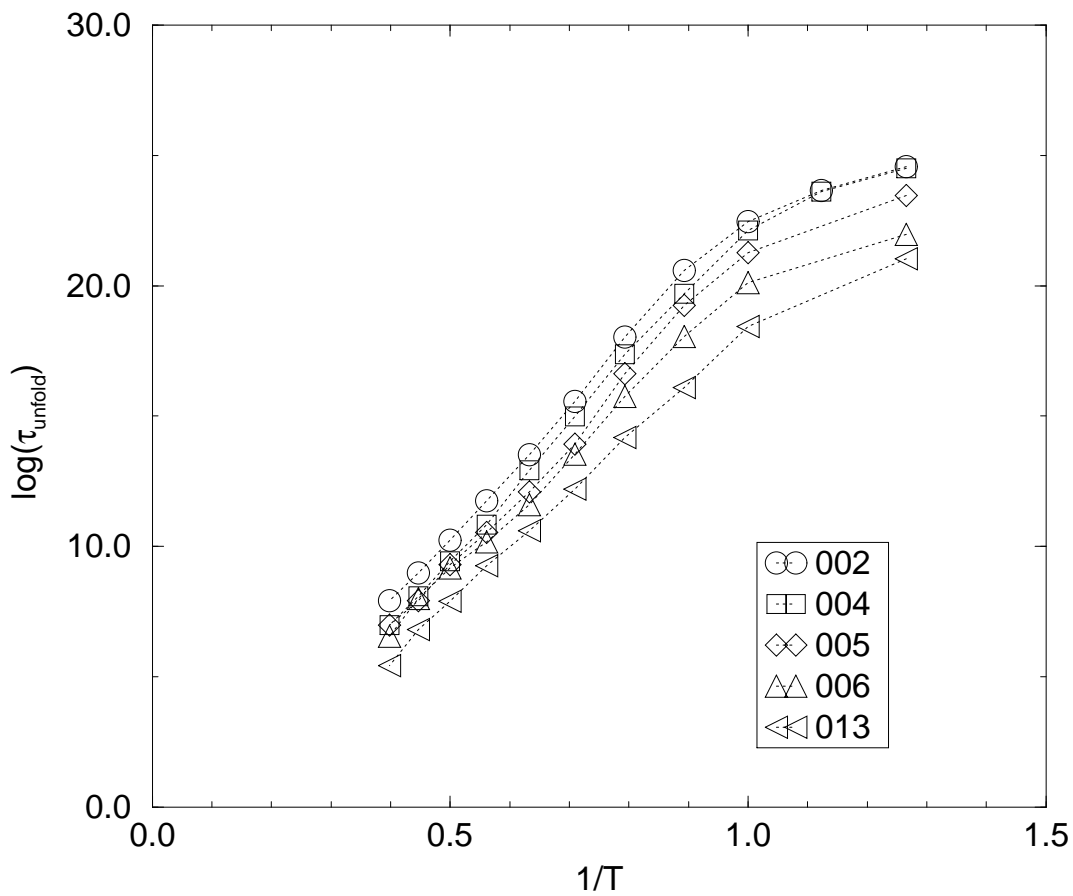
Figure 12: An Arrhenius plot of the unfolding time against the inverse temperature for five of the sequences. The unfolding time was calculated by multiplying the folding time by the ratio of the folded population to the unfolded population at a given temperature. Consequently, there is the same saturation effect at low temperature as in figure 9 caused by the finite simulation time.

shows the dynamical effects as T_g is approached. There is a clear change in the behavior of the activation energy for unfolding near T_g where the curve starts to level off. This behavior reflects the change in dynamics at T_g suggested by the energy landscape analysis. The loss of dynamical flexibility caused by the entropy crisis leads to dynamical reorganization times limited by the entropy of search and the activation energy of the elementary step. (See equation (11)) This analysis of the computer simulation shows many of the ways in which data can be reduced when the thermodynamic dependence of the underlying forces is understood.

VII   Energy Landscape Analysis and Folding Experiments

We now turn to the analysis of some particular proteins that have been studied extensively in the laboratory, lysozyme, chymotrypsin inhibitor, and cytochrome c. Despite the significant work already done on these systems, we believe that there is insufficient data to uniquely classify the mechanisms of folding via our energy landscape framework. However, it is possible to use the existing data to give a flavor of how these ideas can be used in laboratory situations. As we have seen in our discussion of the computer simulations, many qualitative features of experiments, such as curved Arrhenius plots, can be obtained from the energy landscape scenario, and can even be quantified if the underlying driving forces are understood. A considerable difficulty in the experimental studies is that these driving forces are temperature dependent [13]. It is however important to realize that we can separately change the driving force by such devices as the use of denaturant or mutation and separate this effect from those effects which are directly due to the ruggedness of the energy landscape due to thermal energies. Ruggedness is a more nearly self-averaging quantity. A further analysis of this type for specific systems will, we hope, be made soon.[9]

In some ways, the simplest experimental situation occurs for those proteins and conditions which exhibit a Type I folding mechanism. The kinetics in such systems should be simple exponential. These systems have moderate driving forces and are studied in the near equilibrium range near the midpoint of the transition curve. One feature favoring a Type I transition as opposed to a Type II transition is the avoidance of premature collapse. When collapse occurs corresponding changes in the ruggedness of the energy landscape can arise and play a role. Apparently Type I behavior occurs upon the cold denaturation of lysozyme as studied by Chen and Schellman [119, 120]. It is substantially a uniexponential process.

The folding of chymotrypsin Inhibitor 2, an 83 residue monomeric protein with no disulfide bonds, has been studied by Jackson and Fersht [121, 122]. In many respects their experiments resemble a Type I scenario. Jackson and Fersht used fluorescence measurements and scanning microcalorimetry to study the refolding of this protein. The equilibrium denaturation experiments found strong evidence for a simple two-state transition without intermediates. The kinetic measurements, however, reveal three phases, but it is clear that these are due to the five proline residues in the molecule, of which at least four are in the *trans* state in the crystal structure. Seventy-seven percent of the protein molecules fold with a time constant of .02 seconds and the two observable slow phases have time constants of 43 and 500

---

[9]At this point the reader may wish to review the folding scenarios discussed in Figure 5.

seconds. The slow phases are catalyzed by peptidyl-prolyl isomerase, which catalyzes proline isomerization. The fast phase is not affected by this enzyme. The protein molecules that start with all the prolines in the *trans* configuration have very nearly exponential kinetics on the timescale studied.

In the energy landscape view, proline isomerization appears as a high ridge separating the configurations with a *cis* isomer from those with a *trans* isomer [123, 124]. One such ridge appears for each proline in the protein. Each of these separate parts of the configuration space can be analyzed with the simple energy landscape concepts that we have already discussed. Thus, the mere observation of multiexponentiality is not enough to imply that these systems obey Type II kinetics in which a glass transition is present. These ridges in the energy landscape come from the simple effect of single amino acid residues, whereas the glass transition comes from the composite effect of all the amino acid residues in the protein.

An example of apparent Type II behavior in provided by hen lysozyme at its high temperature denaturation transition. The evidence for Type II behavior of lysozyme at this transition is largely based on the CD measurements and pulsed hydrogen-exchange labeling carried out by Radford *et al.* [125]. These studies suggest multi-exponential behavior for the protection of the amide hydrogens, which Radford *et al.* have interpreted as due to the existence of multiple parallel folding pathways. The Type II nature of this transition apparently occurs because of the possibility of early collapse. In addition, misfolding is apparently present since the CD shows, after the first 100 milliseconds, considerably more α-helix present than is present in the native state. Thus, in this situation, the folding protein adopts a locally favorable conformation which must be partly unfolded to get into the globally favored native state. The initial strong local tendency towards helix formation is giving rise to frustration in the technical sense of competing interactions discussed earlier in this paper. The Type II behavior suggests that the roughness of the energy landscape for lysozyme is actually larger, compared to $k_B T$, at the high temperatures than at the low temperatures, apparently due to the temperature dependence of the hydrophobic forces.

Cytochrome c, with its heme constraints, apparently has little roughness to its energy landscape compared to the free energy gradient. The heme is covalently bound to the protein chain and after the iron coordination sphere is completed, folding of different parts of the protein occur rather rapidly. On the other hand, the heme group can also be misligated by some of the amino acids in the protein and this misligation can be detected spectroscopically. The mis-ligated population can not follow the free energy gradient all the way to the native structure so the presence of the heme also facilitates the study of the different mis-folded structures present in an ensemble of folding proteins. Sosnick *et al.* have studied the folding of cyctochrome *c* under conditions where the misligation does not occur [126]. They found that about 50 - 70 % of the molecules in this population acquired native secondary and tertiary structure with a time constant of approximately 15 milliseconds. They estimated, from fluorescence quenching, the time constant for collapse to be approximately 12 milliseconds, that is, the of the same order as the folding time. These experiments suggest that cytochrome *c* folding is Type 0 under these conditions though it is difficult to assign it to Type 0A or Type 0B with the data from these experiments. Experiments on cytochrome *c* folding provide a good illustration of how the folding of a particular protein can vary *qualitatively* as the conditions of the folding experiment vary.

For example, when cytochrome c is refolded at pH 6.2, the folding is multiexponential and takes on the order of seconds. Sosnick *et al.* have also shown that the slow folding at pH 6.2 is due to the formation of a mis-folded, collapsed structure, rather than the specific mis-ligation of the heme, in agreement with the picture of a glassy phase presented here.

VIII   Conclusion

The energy landscape picture allows us to combine various disparate ideas about the nature of biomolecular self-organization in protein folding. The energy landscape picture can accommodate multiple parallel path scenarios, as well as unique, sequence-dependent pathways for protein folding. The crucial concept in understanding particular experimental and computer simulation situations is to organize the kinetics of the problem through the consideration of a phase diagram and to study of the dynamics of the crucial order parameters for folding which distinguish folded states from unfolded ones. In a generic energy landscape picture, several different phase transitions occur and are coupled. At the very minimum, one must consider the two purely thermodynamic transitions of folding and of collapse. The collapse transition temperature depends upon both the overall tendency for self-association and also on the ruggedness of the energy landscape. Above the glass transition collapse is a largely self-averaging process; that is, it depends on the overall composition of the sequence and on little else. The folding transition, on the other hand, is always sensitive to the details of the sequence. In addition to these conventional, understood phases, a rough energy landscape exhibits a glass transition which occurs near a thermodynamic glass transition temperature, T_g. This temperature is also a self-averaging property of different sequences of similar composition.

Different scenarios for protein folding mechanisms occur, depending on the relationship of these various temperatures and the conditions under which the experiment is carried out. The simplest situation to understand occurs when there is a moderate driving force toward the folded state. Near to the midpoint of the denaturation curve, there will be an overall double minimum potential of free energy function and the roughness of the energy landscape simply acts to modulate the rate of passing over the transition state. This transition state is actually a set of many configurations and could be said to consist of numerous micro-transition states in a funnel toward the folded state. The kinetics in this situation are simple exponential. If the driving forces for folding are considerably smaller, the folding temperature can become close to the glass transition temperature. In this case one encounters considerable slowing of the folding process itself; a Type II scenario emerges in which individual pathways for folding can be dissected. Here there will be multiple exponential processes typically. The great irony, of course, is that in the situation where we can find individual pathways, folding will be typically very slow. Indeed, nearly kinetically unfoldable proteins would exhibit the most clearly defined pathway for folding. These discrete pathways, however, are not self-averaging aspects of the dynamics and are sensitive to individual mutations in sequence.

For very large driving forces, one can encounter Type 0 scenario folding in which essentially all of the dynamics goes on in a downhill manner. If a Type 0 scenario can occur much above T_g, this gives rise to processes that are very fast (of order of ordinary homopolymer collapse times) [127]. On the other hand, if the glass transition intervenes, which is likely if

non-specific collapse occurs, individual pathways can still be found, and, again, they will be strongly sequence dependent and sensitive to mutations.

If the qualitative nature of the interaction energy scales is understood, detailed temperature dependences can be obtained by the energy landscape analysis. A typical feature of this analysis is that one obtains curved Arrhenius plots for folding times, much like those actually occurring in experimental situations. This curvature reflects the roughness of the energy scale of the particular protein and enters in both a thermodynamical and dynamical way. The other energy scale is related to the folding temperature itself and to the stability gap in the energy spectrum of kinetically foldable proteins. Simple linear free energy relations between the folding time and the stability gap energy scale are obtained. A most remarkable feature, however, is that there are discontinuities in these relations and in the apparent activated energies themselves as the glass transition is approached. The main difficulty in using energy landscape analysis to interpret laboratory experiments is the temperature dependence of the underlying thermodynamic forces. Still, the self-averaging nature of the roughness energy scales *versus* the specific sequence dependence of the stability gap scale should allow some insight to be obtained in real experiments. The employment of different modes of denaturation will be essential in differentiating these energy scales of the protein folding landscape. One can think of the use of chemical denaturants, such as urea and guanidine, that largely bind to unfolded configurations as primarily affecting the stability gap rather than the roughness energy scale. On the other hand, pressure will strongly effect all solvent mediated forces and thus will correlate with the roughness energy scale [128–131].

Another complexity in laboratory experiments is that there con be multiple order parameters for real proteins, since folded structures differ in several ways from the typical unfolded ones. The point is, however, that there are probably only a few such parameters and a few overall energy scales that are relevant. If the dynamical re-organization timescales for each of these order parameters are similar the many reaction coordinate situation does not differ dramatically from the one effective coordinate picture we have discussed in detail in this paper. If the timescale for different motions differ appreciably, either through local energy barriers or glass transition temperatures that vary with these order parameters, a more complex scenario in which the folding bottleneck is largely independent of the equilibrium free energy barrier can arise. Still the few coordinate generalization of the present analysis would be applicable. Experimentally this situation would resemble Type II or Type 0B one coordinate scenarios, in that multi-exponential kinetics would be prevalent.

The most important additional order parameters are those measuring the degree of collapse, secondary structure, e.g. helical content, and side-chain ordering. The glass transition characteristics depend greatly on collapse, so this is one possible source of decoupling of the bottleneck from the equilibrium free energy barrier [6]. The ruggedness of the energy landscape also can depend on side-chain orientation since some mis-associations may simply not be sterically allowed for some sidechain orientations. In addition, the configurational entropy of the backbone depends on its helical content, again affecting the dynamical glass transition. Certainly in multi-domain proteins one must use different reaction coordinates for each folding unit. Even single domain proteins may have different folding substructures. Some analyses such as that of Bryngelson and Wolynes, suggest that the critical nucleus for folding is large [6] but other studies suggest smaller sizes for the critical nucleus and

concomitantly smaller folding units with separate reaction coordinates [27]. In any case, an energy landscape analysis allows us to reduce, in many circumstances, a huge number of variables down to only a few degrees of freedom and a statistical characterization of the roughness of the energy landscape. The true diversity of the energy landscape only comes through in the Type II scenarios in which the glass transition has intervened. A study of most experiments suggests that many proteins are near to the glass transition and may show Type 0B and Type II scenarios. Since the roughness of the energy scale is self-averaging, it will be interesting to explore the phase diagram for different protein and especially to examine different protein compositional classes to see if there are systematic differences in energy scale roughness in *in vitro* folding.

One of the major fruits of the energy landscape analysis of protein folding has been a simple variational criterion for achieving fast-folding proteins. The minimal frustration principle, which at first seemed a qualitative concept, has been formulated now as a criterion for the maximization of the folding temperature compared to the glass transition temperature. This principle has already been used to reverse engineer proteins to discover correlations that are important in predicting protein structure [83, 84]. In addition, it has been used to design proteins that can fold on reasonable timescales on computers [132]. It will be interesting to see whether the combination of the reverse engineering and engineering approaches will allow the design of kinetically foldable proteins in the laboratory.

IX   Acknowledgments

References

[1] Anfinsen, C. B., Haber, E., Sela, M., White, F. H. The kinetics of formation of native ribonuclease during oxidation of the reduced polypeptide chain. Proc. Natl. Acad. Sci. USA 47:1309-1314, 1961.

[2] Levinthal, C. How to fold graciously. In: "Mossbauer spectroscopy in biological systems." Proceedings of a meeting held at Allerton house, Monticello, Illinios. De-

Brunner, P., Tsibris, J., Munck, E. (eds.) Urbana, IL: University of Illinois Press, 1969:22-24.

[3] Harrison, S. C., Durbin, R. Is there a single pathway for the folding of a polypeptide chain? Proc. Natl. Acad. Sci. USA 82:4028-4030, 1985.

[4] Bryngelson, J. D., Wolynes, P. G. Spin glasses and the statistical mechanics of protein folding. Proc. Natl. Acad. Sci. USA 84:7524-7528, 1987.

[5] Bryngelson, J. D., Wolynes, P. G. Intermediates and barrier crossing in a random energy model (with applications to protein folding). J. Phys. Chem. 93:6902-6915, 1989.

[6] Bryngelson, J. D., Wolynes, P. G. A simple statistical field theory of heteropolymer collapse with application to protein folding. Biopolymers 30:177-188, 1990.

[7] Bairoch, A., Boeckmann, B. The SWISS-PROT protein sequence data bank. Nucl. Acids Res. 20:2019-2022, 1992.

[8] Ghélis, C., Yon, J. "Protein Folding." New York: Academic Press, 1982.

[9] Pain, R. H. (ed.) "Mechanisms of Protein Folding." Oxford: Oxford University Press (IRL Press), 1994.

[10] Pauling, L. C. "General Chemistry." 3rd ed. San Francisco: W. H. Freeman and Company, 1970:381-419.

[11] Lewis, G. N., Randall, M. "Thermodynamics." 2nd ed. revised by Pitzer, K. S., Brewer, L. New York: McGraw-Hill Book Company, 1961:138-144.

[12] Franks, F. The hydrophobic interaction. In: "Water: A Comprehensive Treatise." Franks, F. (ed.), Vol. 4. New York: Plenum, 1975:1-94.

[13] Leikin, S., Rau, D. C., Parsegian, V. A. Direct measurement of forces between self-assembled proteins: Temperature-dependent exponential forces between collagen triple helices. Proc. Natl. Acad. Sci. USA 91:276-280, 1994.

[14] Zwanzig, R., Szabo, A., Bagchi, B. Levinthal's paradox. Proc. Natl. Acad. Sci. USA 89:20-22, 1992.

[15] Leopold, P. E., Montal, M., Onuchic, J. N. Protein folding funnels: A kinetic approach to the sequence-structure relationship. Proc. Natl. Acad. Sci. USA 89:8721-8725, 1992.

[16] Dill, K. A. Folding proteins: Finding a needle in a haystack. Curr. Opinion Struct. Biol. 3:99-103, 1993.

[17] McCammon, J. A., Harvey, S. C. "Dynamics of proteins and nucleic acids." Cambridge: Cambridge University Press, 1987.

[18] Frauenfelder, H., Parak, F., and Young, R. D. Conformational substates in proteins. Ann. Rev. Biophys. Biophys. Chem. 17:451-479, 1988.

[19] Poland, D., Scheraga, H. A. "Theory of Helix-Coil Transitions in Biopolymers." New York: Academic Press, 1970.

[20] Landau, L. D., Lifshitz, E. M. "Statistical Physics, Part 1." 3rd ed. Sykes, J. B., Kearsley, M. J. trans., Course of Theoretical Physics Vol. 5. Oxford: Pergamon Press, 1980:531-537.

[21] Lifshitz, E. M., Pitaevskii, L. P. "Physical Kinetics." Sykes, J. B., Franklin, R. N. trans., Course of Theoretical Physics Vol. 10. Oxford: Pergamon Press, 1981:427-438.

[22] Ma, S.-K. "Statistical Mechanics." Fung, M. K., trans. Singapore: World Scientific Publishing Company, 1985:265-268.

[23] Privalov, P. L. Stability of proteins. Small globular proteins. Adv. Protein Chem. 33:167-241, 1979.

[24] Ginsburg, A., Carroll, W. R. Some specific ion effects on the conformation and thermal stability of ribonuclease. Biochemistry 4:2159-2174, 1965.

[25] Anfinsen, C. B. The formation and stabilization of protein structure. Biochem. J. 128:737-749, 1972.

[26] Nojima, H., Ikai, A., Oshima, T., Noda, H. Reversible thermal unfolding of thermostable phosphoglycerate kinase. Thermostability associated with zero mean enthalpy change. J. Mol. Biol. 116:429-442, 1972.

[27] Thirumalai, D., Guo, Z. Nucleation Mechanism for Protein Folding and Theoretical Predictions for Hydrogen-Exchange Labelling Experiments. preprint, 1994.

[28] Binder, K., Young, A. P. Spin glasses: Experimental facts, theoretical concepts and open questions. Rev. Mod. Phys. 58:801-976, 1986.

[29] Mézard, M., Parisi, G., Virasoro, M. A. "Spin Glass Theory and Beyond." Singapore: World Scientific, 1986.

[30] Fischer, K. H., Hertz, J. A. "Spin Glasses." Cambridge: Cambridge University Press, 1991.

[31] Anderson, P. W. The concept of frustration in spin glasses. J. Less-Common Metals 62:291-294, 1978

[32] Garey, M. R., Johnson, D. S. "Computers and Intractability: A Gouide to the Theory of NP-Completeness." San Francisco: W. H. Freeman and Company, 1979.

[33] Unger, R., Moult J., Finding the Lowest Free Energy Conformation of a Protein is an NP-Hard Problem: Proof and Implications. Bull.Math.Biol. 55: 1183-1198, 1993.

[34] Kirkpatrick, S., Gelatt, C. D. Jr., Vecchi, M. P. Optimization by simulated annealing. Science 220:671-680, 1983.

[35] LaBean, T. H., Kauffman, S. A., Butt, T. R. Libraries of Random-Sequence Polypeptides with High Yield as Carboxy-Terminal Fusions with Ubiquitin. preprint, 1994.

[36] Davidson, A. R., Sauer, R. T. Folded proteins occur frequently in libraries of random amino acid sequences. Proc. Natl. Acad. Sci. 91:2146-2150, 1994.

[37] Branden, C., Tooze, J. "Introduction to Protein Structure." New York: Garland Publishing, 1991. p.62.

[38] Presta, L. G., Rose, G. D. Helix signals in proteins. Science 240:1632-1641, 1988.

[39] Richardson, J. S., Richardson, D. C. Amino acid preferences for specific locations at the ends of α helices. Science 240:1648-1652, 1988.

[40] Camacho, C. J., Thirumalai, D. Kinetics and thermodynamics of folding in model proteins. Proc. Natl. Acad. Sci. USA 90:6369-6372, 1993.

[41] Chan, H. S., Dill, K. A. Transition states and folding dynamics of proteins and heteropolymers. J. Chem. Phys. 100:9238-9257, 1994.

[42] Chan, H. S., Dill, K. A. Energy landscapes and the collapse dynamics of homopolymers, J. Chem. Phys. 99:2116-2127, 1993.

[43] Brawer, S. A. "Relaxation in viscous liquids and glasses." New York: Am. Ceram. Soc., 1983.

[44] Jäckle, J. Models of the glass transition. Rep. Prog. Phys. 49:171-232, 1986.

[45] Derrida, B. Random-energy model: Limit of a family of disordered models. Phys. Rev. Lett. 45:79-82, 1980.

[46] Derrida, B. Random-energy model: An exactly solvable model of disordered systems. Phys. Rev. B 24:2613-2626, 1981.

[47] Gross, D. J., Mézard, M. The simplest spin glass. Nucl. Phys. B 240:431-452, 1984.

[48] Garel, T., Orland, H. Mean-field model for protein folding. Europhys. Lett. 6:307-310, 1988.

[49] Shakhnovich, E. I., Gutin, A. M. Formation of unique structure in polypeptide chains. Theoretical investigation with the aid of a replica approach. Biophys. Chem. 34:187-199, 1989.

[50] Lau, K. F., Dill, K. A. A lattice statistical mechanics model of the conformational and sequence spaces of proteins. Macromolecules, 22:3986-3997, 1989.

[51] Lau, K. F., Dill, K. A. Theory for protein mutability and biogenesis. Proc. Natl. Acad. Sci. USA 87:638-642, 1990.

[52] Chan, H. S., Dill, K. A. "Sequence space soup" of proteins and copolymers. J. Chem. Phys. 95:3775-3787, 1991.

[53] Yue, K., Dill, K. A. Sequence-structure relationships in proteins and copolymers. Phys. Rev. E 48:2267-2278, 1994.

[54] Shakhnovich, E. I., Gutin, A. M. Implications of thermodynamics of protein folding for evolution of primary sequences. Nature 346:773-775, 1990.

[55] Shakhnovich, E. I., Gutin, A. M. Enumeration of all compact conformations of copolymers with random sequence of links. J. Chem. Phys. 93:5967-5971, 1990.

[56] Covell, D. G., Jernigan, R. L. Conformations of folded proteins in restricted spaces. Biochemistry 29:3287-3294, 1990.

[57] Hinds, D. A., Levitt, M. A lattice model for protein structure prediction at low resolution. Proc. Natl. Acad. Sci. USA 89:2536-2540, 1992.

[58] Honeycutt, J. D., Thirumalai, D. Metastability of the folded states of globular proteins Proc. Natl. Acad. Sci. USA 87:3526-3529, 1990.

[59] Honeycutt, J. D., Thirumalai, D. The nature of the folded state of globular proteins. Biopolymers 32:695-709, 1992.

[60] Scheraga, H. A. Influence of interatomic interactions on the structure and stability of polypeptides and proteins. Biopolymers 20:1877-1899 (1981)

[61] Jones, C. M., Henry, E. R., Hu, Y., Chan, C.-K., Luck, S. D., Bhuyan, A., Roder, H., Hofrichter, J., Eaton, W. A. Fast events in protein folding initiated by nanosecond laser photolysis. Proc. Natl. Acad. Sci USA 90:11860-11864, 1993.

[62] O'Shea, E. K., Klemm, J. D., Kim, P. S., Alber, T. X-ray structure of the GCN4 leucine zipper, a two-stranded, parallel coiled coil. Science 254:539-544, 1991.

[63] Gō, N. Theoretical studies of protein folding. Ann. Rev. Biophys. Bioeng. 12:183-210, 1983.

[64] Schulz, G. E., Schirmer, R. H. "Principles of Protein Structure." New York: Springer-Verlag, 1979:147-148.

[65] Creighton, T. E. "Proteins." New York: W. H. Freeman and Company, 1984:231.

[66] Flory, P. J. The configuration of real polymer chains. J. Chem. Phys. 17:303-310, 1949.

[67] Flory, P. J. "Principles of Polymer Chemistry." Ithaca, New York: Cornell University Press, 1954:523-530.

[68] Ptitsyn, O. B. The molten globule state. In: "Protein folding." Creighton, T. E. (ed.), New York: W. H. Freeman and Company, 1992:243-300.

[69] Glasstone, S., Laidler, K. J., Eyring, H. "The theory of rate processes." New York: McGraw-Hill, 1941.

[70] Moore, J. W., Pearson, R. G. "Kinetics and Mechanism." New York: John Wiley and Sons, 1981:137-191.

[71] Šali, A., Shakhnovich, E., Karplus, M. How does a protein fold? Nature 369:248-251, 1994

[72] Ferry, J. D., Grandine, E. R., Fitzgerald, E. R. Viscoelastic relaxation of polyisobuty-lene. J. Appl. Phys. 24:911-921, 1953.

[73] Creighton, T. E. The protein folding problem. In: "Mechanisms of Protein Folding." Pain, R. H. (ed.) Oxford: Oxford University Press (IRL Press), 1994:1-25.

[74] Rao, S. P., Carlstrom, D. E., Miller, W. G. Collapsed structure polymers: A scatter-gun approach to amino acid copolymers. Biochemistry 13:943-952, 1974.

[75] Oxtoby, D. New perspectives on freezing and melting. Nature 347:725-730, 1990.

[76] Kim, P. S., Baldwin, R. L. Specific intermediates in the folding reactions of small proteins and the mechanism of protein folding. Ann. Rev. Biochem. 51:459-489, 1982.

[77] Lesk, A. M., Rose, G. D. Folding units in globular proteins. Proc. Natl. Acad. Sci. USA 78:4304-4308, 1981.

[78] Karplus, M., Weaver, D. L. Protein-folding dynamics. Nature 260:404-406, 1976.

[79] Karplus, M., Weaver, D. L. Diffusion-collision model for protein folding. Biopolymers 18:1421-1437, 1979.

[80] Weaver, D. L. Microdomain dynamics in folding proteins. Biopolymers 21:1275-1300, 1982.

[81] Weaver, D. L. Alternative pathways in diffusion-collision controlled protein folding. Biopolymers 23:675-694, 1984.

[82] Karplus, M., Weaver, D. L. Protein folding dynamics: The diffusion-collision model and experimental data. Protein Sci. 3:650-668, 1994.

[83] Goldstein, R. A., Luthey-Schulten, Z. A., Wolynes, P. G. Optimal protein-folding codes from spin-glass theory. Proc. Natl. Acad. Sci. USA 89:4918-4922, 1992.

[84] Goldstein, R. A., Luthey-Schulten, Z. A., Wolynes, P. G. Protein tertiary structure recognition using optimized Hamiltonians with local interactions. Proc. Natl. Acad. Sci. USA 89:9029-9033, 1992.

[85] Karplus, M., McCammon, J. A. Dynamics of proteins: Elements and function. Ann. Rev. Biochem. 53:263-300, 1983.

[86] Šali, A., Shakhnovich, E., Karplus, M. Kinetics of protein folding. A lattice model study of the requirements for folding to the native state. J. Mol. Biol. 235:1614-1636, 1994.

[87] Rooman, M. J., Kocher, J.-P. A., Wodak, S. J. Extracting information on folding from the amino acid sequence: Accurate predictions for protein regions with preferred conformation in the absence of tertiary information. Biochemistry, 31:10226-10238, 1992.

[88] Kolinski, A., Skolnick, J. Monte Carlo simulations of protein folding. I. Lattice model and interaction scheme. Proteins 18:338-352, 1994.

[89] Kolinski, A., Skolnick, J. Monte Carlo simulations of protein folding. II. Application to protein A, ROP and crambin. Proteins 18:353-366, 1994.

[90] Socci, N. D., Onuchic, J. N. Folding kinetics of protein-like heteropolymers. J. Chem. Phys. 101:1519-1528, 1994.

[91] Taketomi, H., Ueda, Y., Gō, N. Studies on protein folding, unfolding and fluctuations by computer simulation. I. The effect of specific amino acid sequence represented by specific inter-unit interactions. Int. J. Pept. Protein Res. 7:445-459, 1975.

[92] Gō, N., Taketomi, H. Respective roles of short- and long-range interactions in protein folding. Proc. Natl. Acad. Sci. USA 75:559-563, 1978.

[93] Abe, H., Gō, N. Noninteracting local-structure model of folding and unfolding transition in globular proteins. II. Application to two-dimensional lattice proteins. Biopolymers 20:1013-1031, 1980.

[94] Kanô, F., Gō, N. Dynamics of folding and unfolding transition in a globular protein studied by time correlation functions from computer simulations. Biopolymers 21:565-581, 1981.

[95] Miyazawa, S., Jernigan, R. L. Equilibrium folding and unfolding pathways for a model protein. Biopolymers 21:1333-1363, 1982.

[96] Kolinski, A., Skolnick, J., Yaris, R. Monte Carlo simulations on an equilibrium globular protein folding model Proc. Natl. Acad. Sci. USA 83:7267-7271, 1986.

[97] Skolnick, J., Kolinski, A. Simulations of the folding of a globular protein. Science 250:1121-1125, 1990.

[98] Kolinski, A., Milik, M., Skolnick, J. Static and dynamic properties of a new lattice model of polypeptide chains. J. Chem. Phys. 94:3978-3985.

[99] Skolnick, J., Kolinski, A. Dynamic Monte Carlo simulations of a new lattice model of globular protein folding, structure and dynamics. J. Mol. Biol. 212:819-836, 1990.

[100] Rey, A., Skolnick, J. Comparison of lattice monte carlo dynamics and brownian dynamics folding pathways of the α-helical hairpins. Chem. Phys. 158:199-219, 1990.

[101] Skolnick, J., Kolinski, A. Computer simulations of globular protein folding and tertiary structure. Annu. Rev. Phys. Chem. 40:207-235, 1989.

[102] Chan, H. S., Dill, K. A. Polymer principles in protein structure and stability. Annu. Rev. Biophys. Biophys. Chem. 20:447-490, 1991.

[103] Guo, Z., Thirumalai, D., Honeycutt, J. D. Folding kinetics of proteins: A model study. J. Chem. Phys. 97:525-535, 1992.

[104] Covell, D. G. Lattice model simulations of polypeptide chain folding. J. Mol. Biol. 235:1032-1043, 1994.

[105] Shakhnovich, E., Farztdinov, G., Gutin, A. M., Karplus, M. Protein folding bottlenecks: A lattice Monte Carlo simulation. Phys. Rev. Lett. 67:1665-1668, 1991.

[106] Flanagan, J. M., Kataoka, M., Fujisawa, T., Engelman, D. M., Mutations can cause large changes in the conformation of a denatured protein. Biochemistry 32:10359-10370, 1993.

[107] Miller, R., Danko, C. A., Fasolka, J., Balazs, A. C., Chan, H. S., Dill, K. A. Folding kinetics of proteins and copolymers. J. Chem. Phys. 96:768-780, 1992.

[108] Berry, R. S., Rice, S. A., Ross, J. "Physical Chemistry." New York: John Wiley and Sons, 1980:1165-1167.

[109] Leffler, J. E., Grunwald, E. "Rates and Equilibria of Organic Reactions" New York: John Wiley and Sons, 1963:156-161.

[110] Wells, P. R., "Linear Free Energy Relationships." New York: Academic Press, 1968.

[111] Matthews, C. R. Effect of point mutations on the folding of globular proteins. Meth. Enzymol. 154:498-511, 1987.

[112] Matouschek, A., Fersht, A. R. Protein engineering in analysis of protein folding pathways and stability. Meth. Enzymol. 202:82-112, 1987.

[113] Jennings, P. A., Saalau-Bethell, S. M., Finn, B. E., Chen, X., Matthews, C. R. Mutational analysis of protein folding mechanisms. Meth. Enzymol. 202:113-126, 1991.

[114] Matouschek, A., Serrano, L., Fersht, A. R. Analysis of protein folding by protein engineering. In: "Mechanisms of Protein Folding." Pain, R. H. (ed.) Oxford: Oxford University Press (IRL Press), 1994:137-159.

[115] Szabo, A. The kinetics of hemoglobin and transition state theory. Proc. Natl. Acad. Sci. USA 75:2108-2111, 1978.

[116] Schellman, J. A. Solvent denaturation. Biopolymers 17:1305-1322, 1978.

[117] Eaton, W. A., Henry, E. R., Hofrichter, J. Application of linear free energy relations to protein conformational changes: The quaternary structural change of hemoglobin. Proc. Natl. Acad. Sci. USA 88:4472-4475, 1991.

[118] Leffler, J. E. Parameters for the Description of the Transition State. Science 117:340-341, 1953.

[119] Chen, B.-Z., Schellman, J. A. Low-temperature unfolding of a mutant of phage T4 lysozme. 1. Equilibrium studies. Biochemistry, 28:685-691, 1989.

[120] Chen, B.-Z., Baase, W. A., Schellman, J. A. Low-temperature unfolding of a mutant of phage T4 lysozme. 2. Kinetic investigations. Biochemistry, 28:691-699, 1989.

[121] Jackson, S. E., Fersht, A. R. Folding of chymotrypsin inhibitor 2. 1. Evidence for a two-state transition. Biochemistry 30:10428-10435, 1991.

[122] Jackson, S. E., Fersht, A. R. Folding of chymotrypsin inhibitor 2. 2. Influence of proline isomerization on the folding kinetics and thermodynamic characterization of the transition state of folding. Biochemistry 30:10436-10443, 1991.

[123] Nall, B. T. Proline isomerization and folding of yeast cytochrome c. In:"Protein Folding: Deciphering the Second Half of the Genetic Code." Washington, D. C.: AAAS, 1990:198-207.

[124] Nall, B. T. Proline isomerization as a rate-limiting step. In: "Mechanisms of Protein Folding." Pain, R. H. (ed.) Oxford: Oxford University Press (IRL Press), 1994:137-159.

[125] Radford, S. E., Dobson, C. M., Evans, P. A. The folding of hen lysozyme involves partially structured intermediates and multiple pathways. Nature 358:302-307, 1992.

[126] Sosnick, T. R., Mayne, L., Hiller, R., Englander, S. W. The barriers in protein folding. Nature Struct. Biol. 1:149-156, 1994.

[127] de Gennes, P. G. Kinetics of collapse for a flexible coil. J. Physique Lett. 46:L-639 - L-642, 1985.

[128] Zipp, A., Kauzmann, W. Pressure denaturation of metmyoglobin. Biochemistry 12:4217-4228.

[129] Li, T. M., Hook, J. W. III., Drickamer, H. G., Weber, G. Plurality of pressure denatured forms lysozyme and chymotrypsinogen. Biochemistry 15:5571-5580.

[130] Samarasinghhe, S. D., Campbell, D. M., Jonas, A., Jonas, J. High-resolution NMR study of the pressure-induced unfolding of lysozyme. Biochemistry 31:7773-7778, 1992.

[131] Royer, C. A., Hinck, A. P., Loh, S. N., Prehoda, K. E., Peng, X., Jonas, J., Markley, J. L. Effects of amino acid substitution on the pressure denaturation of staphylococcal nuclease as monitored by fluorescence and nuclear magnetic resonance spectroscopy. Biochemistry 32:5222-5232, 1993.

[132] Shakhnovich, E. I., Gutin, A. M. Engineering of stable and fast-folding sequences of model proteins. Proc. Natl. Acad. Sci. USA 90:7195-7199, 1993.